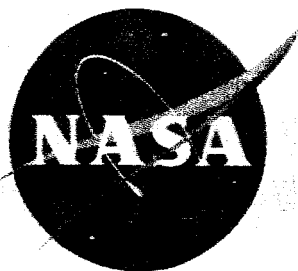
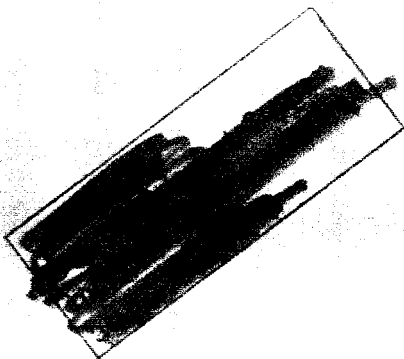


NASA TM X-718



CATEGORY
SPECIAL HANDLING
CASE FILE
COPY

TECHNICAL MEMORANDUM

X-718

WEIGHTLESSNESS EXPERIMENTS WITH LIQUID HYDROGEN

IN AEROBEE SOUNDING ROCKETS; UNIFORM

RADIANT HEAT ADDITION - FLIGHT 2

By Jack G. McArdle, Richard C. Dillon,
and Donald A. Altmos

Lewis Research Center
Cleveland, Ohio

Declassified by authority of NASA
Classification Change Notices No. 143
Dated ** 2-14-68



NATIONAL AERONAUTICS AND SPACE ADMINISTRATION

WASHINGTON

December 1962



[REDACTED]

NATIONAL AERONAUTICS AND SPACE ADMINISTRATION

TECHNICAL MEMORANDUM X-718

WEIGHTLESSNESS EXPERIMENTS WITH LIQUID HYDROGEN

IN AEROBEE SOUNDING ROCKETS; UNIFORM

RADIANT HEAT ADDITION - FLIGHT 2*

By Jack G. McArdle, Richard C. Dillon,
and Donald A. Altmos

SUMMARY

The behavior of a 9-inch-diameter spherical tank 32 percent filled with liquid hydrogen with uniform radiant-heat addition during flight is described. The maximum attainable period of weightlessness was not realized. At various times, the experiment was subjected to oscillatory, spinning, and near-perfect weightless environments. Good telemetered data for the entire flight and some photographs of the hydrogen were obtained. Data indicate that the liquid tends to cling to the container wall and move with it during spinning. The hydrogen was not in thermal equilibrium throughout the flight. The heat-transport process within the liquid may be similar to subcooled nucleate boiling.

INTRODUCTION

Details of the behavior of fluids during simultaneous conditions of weightlessness and heat addition are of concern for space flight because any liquid that is stored for a time in space will absorb heat from surrounding structures and from the sun and planets. It is therefore necessary to incorporate features in the vehicle that allow for fluid heating, vaporization, pressurization, venting, and the like. Conventional earth tests, in many instances, will not yield the correct design information, because gravitational effects mask forces that become controlling during weightlessness. Both analytical and experimental studies of fluids in a weightless environment may be found in references 1 to 7.

The Lewis Research Center is currently engaged in a broad study of fluid behavior in a reduced-gravity environment. The program includes

*Title, Unclassified.

[REDACTED]

experiments in rockets, in drop towers, and in airplanes flying parabolic trajectories.

This report describes the second of a series of Aerobee 150A sounding-rocket flights in which a partly filled tank of liquid hydrogen is carried. This payload was essentially the same as for the first flight in the series (ref. 8), except that the rocket casing was despun after burnout to eliminate payload oscillations. The experiment consisted of a 9-inch-diameter spherical partly filled (32 percent) tank of liquid hydrogen that was subjected to a uniform radiative heat input about equal to the maximum solar input to an unshielded stainless-steel tank in an earth orbit. Instrumentation measured vehicle performance, tank wall temperature, pressure rise, and heat addition. A recoverable camera was used to obtain pictures of the liquid hydrogen during flight.

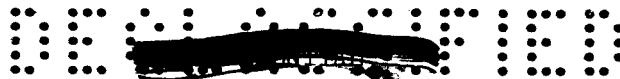
The objectives of this flight were (1) to further evaluate the Aerobee as a "zero-g" facility, and (2) to obtain data on liquid hydrogen in a low-gravity environment. A detailed description of the Aerobee rocket as a low-gravity test facility is given in reference 8.

APPARATUS

Figure 1 is a sketch of the spin-stabilized free-flight rocket and payload showing the relative locations of major components. The only change made to the Aerobee was the addition of subsystems to provide additional thrust after burnout and to despin the rocket casing at a programmed time. The aft section of the payload was fixed to the rocket. The remaining apparatus, hereinafter termed the "experiment," was mounted on a spin-rate-regulated turntable to prevent spinning.

A cross-sectional sketch of the liquid-hydrogen Dewar is shown in figure 2. This Dewar is the same as that used in the test of reference 8 (see ref. 8 for a complete description and discussion) except that the instrumentation leads, for the sphere in this report, were made of constantan. The heater shell was made in two halves to permit assembly. Facing surfaces of the heater and the liquid-hydrogen sphere were sprayed, after instrumenting, with about 0.002 inch of dull black lacquer. The leads to the liquid-hydrogen sphere temperature transducers were secured to the sphere wall at frequent intervals. The fill and vent tubes were machined of stainless steel in such a way that heat conduction was reduced to a practical minimum. Additional design details and materials are indicated in figure 2.

The heater temperature controller was designed to bring the heater to the 575° R set-point temperature as quickly as possible. Power was supplied to the heater by the controller through on-off solid-state switches.



INSTRUMENTATION

Data was telemetered (PPM/AM) to and photographically recorded at a ground station near the launching tower.

Flight Performance

The trajectory was determined by radar. Longitudinal acceleration was measured with one -1 g to +15 g accelerometer and two ± 0.01 g accelerometers. Attitude and spin rate were determined by three magnetometers on mutually perpendicular axes and by two sun sensors. Rocket chamber-, despin nozzle-, and antirag-nozzle-pressures, and turntable performance parameters were measured.

Experiment Performance

Spin relative to the rocket was detected by a potentiometer bracketed between sections of the turntable. Temperatures were measured by 19 small flat platinum resistance-type transducers on the liquid-hydrogen sphere and by three on the heater shell. Locations of the sphere transducers are listed in table I. Hydrogen pressure was measured by a 0 to 50 and a 0 to 200 pound-per-square-inch-absolute transducer. The liquid level was determined by a calibrated height scale inside the sphere (see fig. 2) plus optical readout accessories for ground use prior to launch. Hydrogen boiloff between the time of the last visual reading and liftoff was measured with a laboratory displacement-type gas meter. A 35-millimeter double-frame camera, with optics that provided a 90° field of view, was operated with a strobe light source at 5 frames per second. A signal was telemetered each time the film advanced so that a correlation could be made between photographic and telemetered data.

PROCEDURE

The experiment was mounted on a turntable designed to prevent spinning in order to minimize liquid-hydrogen motions; however, because of a malfunction, some spinning did occur. Additional thrust was provided after sustainer burnout to approximately overcome air drag; this was done to reduce liquid-hydrogen splashing. The rocket was despun at near-zero air drag and then allowed to coast for about $2\frac{1}{2}$ minutes. A small thrust was produced for a short time just before atmospheric reentry in an effort to collect and mix the liquid hydrogen.

The Dewar was cooled with cryogenic liquids for several hours prior to installation in the rocket. Liquid nitrogen flowed in the cooling coils until rocket liftoff. A valve in the Dewar vent line was closed



at liftoff, and the quantity of liquid hydrogen in the sphere was calculated with the use of prelaunch boiloff data. Heat transfer was calculated with classical steady-state radiation and conduction equations modified as necessary to apply to the apparatus used. (A complete statement of equations, physical properties, sample calculations, and comparisons of calculated and ground-measured pressure rise in a similar Dewar are given in ref. 8.)

Photographs of liquid motions were correlated, wherever possible, with telemetered pressure and temperature data. In a few cases, photographs from later flights in the series (which had become available at the time of this writing) were used to aid interpretation.

RESULTS AND DISCUSSION

Rocket Performance

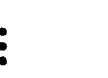
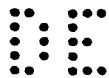
Applicable details of the rocket performance are discussed in appendix A, and a synopsis of the flight is given in table II.

Experiment Performance

Liquid-hydrogen level. - Ninety-seven percent para-hydrogen was used. The prelaunch boiloff rate is shown in figure 3. From this curve and from the last visual reading, the sphere was calculated to contain 32 percent liquid hydrogen by volume at liftoff. This is equivalent to 0.31 pound liquid hydrogen plus 0.013 pound hydrogen vapor, 4.0 percent quality, 1.47 pounds per cubic foot system density (defined as the total hydrogen weight divided by the container volume).

Spin rate. - The turntable operated properly until 186 seconds. After that time, an electrical failure caused the experiment to spin (see fig. 4). During the first spin period, from 186 to 199 seconds, the experiment accelerated and decelerated rapidly. During the second period, it accelerated rapidly but decelerated more gradually because of complete loss of electrical power. The spin rate became zero after the collection process was completed.

Lateral accelerations. - As the rocket was despun, the lateral accelerometer output, as shown in the sketch in figure 5, was similar to that of the first flight in this series. These "oscillations" were probably caused by the line connecting the centers of gravity of the spinning rocket and nonspinning experiment not being coincident with the rocket spin axis either because of unbalance in the rocket or because of mal-alinement of the bearing joining the rocket and the experiment, or both. In that event the centerline of the experiment would move around the surface of a cone that has its apex at the center of gravity of the whole system (which lies within the rocket). Thus, the accelerometers, being



nearer the nose, would experience more centrifugal force than the liquid-hydrogen Dewar. The peak-to-peak amplitude of the oscillation in the plane through the middle of the Dewar is shown in figure 5. These results were calculated with the assumption that centrifugal force varies linearly with distance from the center of gravity of the whole system. There was no measurable lateral acceleration when neither the rocket nor the experiment was spinning.

The lateral accelerometers were forced off scale when the experiment spun. The computed radial acceleration on the experiment caused by spinning only is shown in figure 6; the maximum acceleration that occurred on the liquid-hydrogen sphere was more than 2 g's.

Liquid-Hydrogen Dewar Temperature

Typical faired hydrogen sphere wall-temperature histories are shown in figure 7. (The data and method of correction are presented in appendix B.) Before sustainer burnout the liquid hydrogen is in a pool on the bottom of the sphere. The "wet" portions of the wall are near T_{sat} , the saturation temperature corresponding to the existing hydrogen pressure, while the "dry" portions are much warmer. Just after sustainer burnout the liquid hydrogen washed the whole inside surface of the sphere, which caused the dry walls to cool quickly (fig. 7(a)). When the experiment spun, the walls near the spin axis sometimes became warm. In general, most of the wall was near T_{sat} throughout the coasting portion of the flight. Cases in which the wall was considerably warmer are discussed in detail in the section Fluid Motions.

Evidence of Nucleate Boiling

Nucleate boiling was observed visually with liquid hydrogen in ground tests of a sphere identical to the one used in this experiment at heating rates of about 100 Btu per hour per square foot. In addition, photographs from weightless periods of a later Aerobee flight show what are thought to be bubbles breaking the liquid-hydrogen surface at a heating rate of about 75 Btu per hour per square foot. It is therefore concluded that nucleate boiling occurred during the present test for all heating rates greater than 100 Btu per hour per square foot (or, in other words, at all times after the beginning of despin at 120 sec). Discussion in the following sections is based on this conclusion in some instances. Boiling is discussed in detail in the section on Heat-Transport Mechanism.

Fluid Motions

A photograph taken inside of the liquid-hydrogen Dewar prior to launch is shown in figure 8(a). Useful details are noted for studying



this photograph and those following. Notice particularly that the view is considerably distorted because of the wide-angle optics. Refer to figure 2 for aid in orientation.

Close inspection of figure 8(a) shows small particles in the liquid, which are probably frozen impurities introduced with the hydrogen when the Dewar was filled. Unpublished results of work at this laboratory have determined that foreign elements, such as nitrogen and xenon, are sometimes observed in liquid-hydrogen Dewars.


Figure 8(b) shows the sphere during sustainer burning. The liquid surface is now disturbed by rocket-generated noise. The white substance at the bottom of the sphere is an agglomeration of the particles seen in figure 8(a).

The sustainer motor burned out at about 52 seconds, and despin was not begun until 120 seconds. In the intervening time, the rocket was spinning at a constant rate, and the experiment was oscillating but not spinning. The photographs show, when viewed as movies, that the liquid hydrogen swirled toward the top of the sphere and effectively washed the whole inside wall. Figures 8(c) and (d) were taken at 80 and 110 seconds after liftoff, respectively, and are typical of the pictures obtained. The swirling action, apparent from the motion of the frozen particles, was reduced by the time detail became less apparent (see fig. 8(d)) as the liquid covered the camera port. Since swirling is probably associated with rocket spin and since it is diminishing before despin starts, it is reasonably assumed that swirling is negligible when despin is completed and therefore does not affect fluid motions later in the flight. This conclusion is supported by pictures obtained from a later flight in the series, in which swirling was seen to damp out and disappear under similar conditions.

The bright streaks in figure 8(c) are specular reflections and do not necessarily denote crests of surface waves, although their movement does mean that the surface is disturbed. The source of disturbance has not been isolated. Photographs from a later flight are similar, and it is likely that a great deal of disturbance is caused by bubbles forming, growing, and breaking through the liquid-vapor interface.

The photographs shown in figure 8(e) were taken at 116 seconds after liftoff. An electrical failure caused the strobe light to dim, but the visible details are about the same as in figure 8(d).

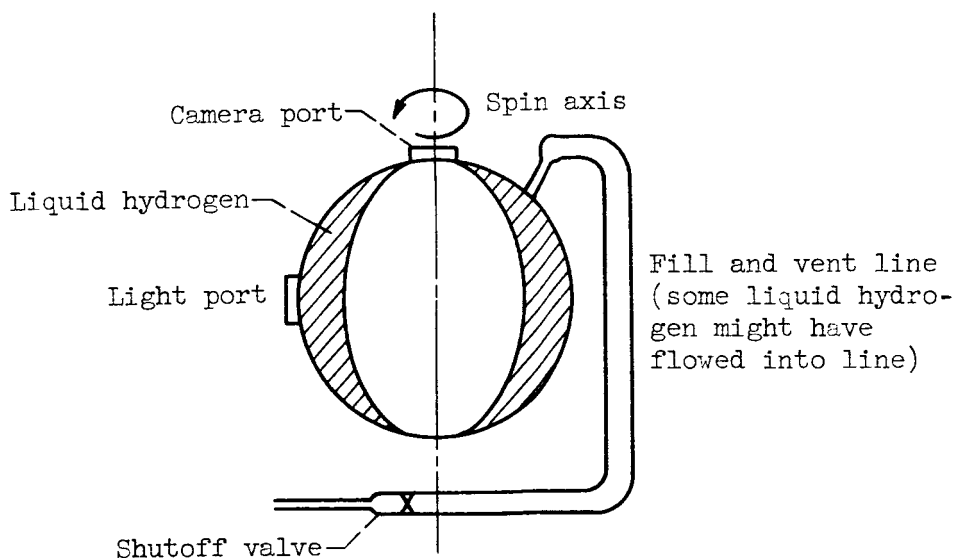
Despin began at 120 seconds, and the pictures in figure 8(f) were taken at 138 seconds when despin was about half completed. By this time, the light source was almost inoperative. The light-port image did not change size and shape as rapidly as it did previously, which could indicate that the liquid was becoming more quiescent.





Near-perfect weightlessness was attained between 166 and 186 seconds, and, as mentioned previously, all liquid motions initially caused by the rocket have probably disappeared. Figures 8(g) and (h) were obtained during this time. Only the light port and highlights around it, which no longer move quickly, can be seen (i.e., compare with fig. 8(d)). Although no proof of the liquid configuration is available from these pictures, it can be deduced from the wall-temperature data and the results of other investigations that the liquid clung to the wall more or less uniformly leaving a single large vapor bubble at the center.

At 186 seconds, both the rocket and the experiment suddenly began to spin. Photographs obtained shortly after that time are of about the same quality as those taken at 180 seconds (fig. 8(h); however, when viewed as movies, the pictures showed plainly that the highlights moved quickly in a clockwise direction. (The photographs are not shown herein, because the motion is very difficult to follow from a series of prints). At the same time the highlights moved, the hydrogen pressure dropped (see fig. 12) and the top of the sphere dried (see fig. 7(a)). These facts indicate that the liquid hydrogen was rearranged by the spinning and was probably beginning to form the configuration shown in the following sketch:



At 194 seconds, the spin rate was 1.9 revolutions per second and the photographs were similar to those in figures 8(g) and (h). The high-lights moved in almost a random fashion, and none were observed to move rapidly. This could indicate that the bulk of the liquid hydrogen was already spinning with the sphere (recall that the camera, too, was spinning). Unfortunately, the light source failed completely at that time, so further information about fluid motion can only be deduced from other instrumentation.

At 199 seconds all spinning quickly stopped, and the top of the sphere suddenly cooled. Spinning occurred again between 215 and 325 seconds. Shortly after 215 seconds the top and bottom sphere walls dried, and the liquid again probably spun at nearly the same rate as the experiment. It is possible that the tendency of the liquid to rotate is increased because boiling makes the wall surface appear "rough."


The collection nozzles were opened at 310 seconds and furnished about 0.01-g longitudinal acceleration for about 8 seconds. For a later flight in which the experiment did not spin, the 0.01-g acceleration was sufficient to drive all the liquid hydrogen to the bottom of the sphere. However, in this flight the only certain effect of the thrust was to hasten cooling of the lower part of the wall (it was already cooling because the spin rate was decreasing). This is additional evidence that the liquid was spinning with the wall, because longitudinal acceleration was small compared with the possible radial acceleration at that time.

Heat Transfer and Hydrogen Pressure

Heater temperature. - Power was applied to the heaters at 40 seconds. The upper- and lower-heater-shell temperature histories are shown in figure 9.

Heat transferred. - The heat-transfer rate is herein considered to be the total heat per unit time absorbed by the hydrogen mass. The computing method is essentially the same as that described in detail in reference 8. The heat-transfer rate from 40 to 350 seconds is shown in figure 10(a). The local peak near 50 seconds is caused by the liquid hydrogen splashing the warm upper portion of the sphere. The heat-transfer rate is about 235 Btu per hour after 140 seconds, of which only about 4 Btu per hour is due to conduction through the support structure and instrumentation leads. This amounts to a uniform heat flux of 132 Btu per hour per square foot for the tank use.

The heat input is the time integral of the heat-transfer rate and is shown in figure 10(b). This computation was arbitrarily started at 40 seconds; at 350 seconds 16.75 Btu, which is equivalent to 51.5 Btu per pound, had been added to the hydrogen.





DECLASSIFIED

Hydrogen pressure. - The measured hydrogen pressure is shown in figure 11; a plot of the experiment spin rate is included for reference. The pressure rose slowly at first, then more rapidly as the heater reached set temperature. Shortly after the experiment first began to spin, the pressure suddenly dropped because the hydrogen mixed. During the rest of the first spin sequence, the pressure was nearly constant, thus, mixing must have continued (heat was added continuously, and the spin rate was always changing). The pressure increased again when the spinning stopped. Behavior was similar at the beginning of the second spin period; then, however, the pressure increased when the spin became almost constant. In general, the pressure history and the available photographs indicate that the boiling liquid (or, at least, a significant liquid layer) requires little time to begin to move with the container wall.

The same pressure data is shown again in figure 12 as a function of the calculated heat input; data from reference 8 is included for comparison. The dot-dash curves represent the pressure that would have been attained if the hydrogen were always in thermal equilibrium. These curves were computed using thermodynamic properties from reference 9 and the amount of hydrogen in the sphere. The measured pressure is always greater than the corresponding computed equilibrium pressure, which shows that the liquid-vapor interface that dictates system pressure is at a greater temperature than T_{equil} , the temperature if hydrogen were in thermal equilibrium. There must be, therefore, some liquid in the container at a lower temperature than T_{equil} (i.e., some liquid must be subcooled). The subcooling, indicated in figure 13 as the difference between the two curves, was small but was present throughout the flight. The temperature gradient in the liquid hydrogen (see sketch in fig. 13) is of unknown shape and magnitude.

Heat-transport mechanism. - The mechanism by which heat is distributed within and absorbed by the enclosed hydrogen is not yet fully understood. Analysis is complicated by the transient nature of the process. Little general information is available in the literature, and classical thermodynamic methods are not applicable because of nonequilibrium.

As noted previously, nucleate boiling was visually observed during ground tests, and photographs of what is probably boiling were obtained during weightlessness in a later Aerobee flight. In each case, the heat-transfer rate was less than the steady-state rate for the present test, and on these bases it has heretofore been assumed that boiling occurred in the present test after 120 seconds. The following paragraphs examine the validity of this assumption in detail.

It has been stated previously that most of the wall was liquid-wetted throughout the coasting portion of the flight. A comparison



03:11:28:10:30

of the average liquid-wetted-wall temperature, which is probably accurate to $\pm 2^\circ \text{R}$ (see appendix B), and T_{sat} is shown in figure 14. Note that the liquid-wetted-wall temperature is very nearly equal to T_{sat} even when portions of the wall are dry and relatively hot. This is taken to be further evidence that boiling occurred, for reference 8 reported similar results and, on the basis of several temperature-difference calculations, concluded that the only basic mechanism that could reasonably account for those results is nucleate boiling or an equivalent action. Another paper (ref. 10) shows that boiling can occur in liquid hydrogen during weightlessness for the heat-transfer rate used in the test of reference 8.

It should be noted here that the present test differed from that of reference 8 in that the heat-transfer rate of reference 8 is about double that of the present test and that the experiment was oscillating, but not spinning, throughout the flight. The difference in heat-transfer rates does not change the results of the calculations of reference 8, but the spinning introduces the possibility that convection is the predominant heat-transport process. (During weightlessness, no convection could occur because of the lack of motion and buoyancy, and, during the oscillating period, the convection forces must have been quite small.) Extensive additional calculations (not presented herein) based on the data of figure 14 have shown that when the sphere is spinning a forced-convection process will account for the heat-transfer rate if it is assumed that the bulk of liquid is not spinning. However, from all the evidence indicating that the liquid moves with the sphere wall and clings to it, apparently, forced convection, if present at all, merely acts in addition to the boiling process. On the other hand, if there is no relative motion between the liquid and the spinning sphere (i.e., if they spin together), free convection cannot account for the measured heat-transfer rate, so, again, boiling must be present. In summation, boiling should have occurred in whatever combination of basic heat-transport processes were involved in this test. Because there was always subcooled liquid in the container, the process may have been similar to subcooled nucleate boiling (sometimes called "local" boiling).

CONCLUDING REMARKS

An experiment to determine the behavior of a partly filled Dewar of liquid hydrogen, under simultaneous conditions of weightlessness and uniform radiant-heat addition, was flown on an Aerobee 150A sounding rocket. Apogee was 95 statute miles, and the rocket with a 303-pound payload could have provided over 4 minutes of near-perfect weightlessness. However, as a result of necessary operational functions (despin, etc.) and an equipment malfunction, only about 20 seconds of near-perfect weightlessness was realized. Throughout the rest of the coasting portion of the flight, the experiment was spinning or oscillating due to rocket-casing spin.

█

DECLASSIFIED

11

After sustainer burnout, the liquid-hydrogen container walls were liquid-wetted except near the spin axis when the container was spinning. The average liquid-wetted-wall temperature was always nearly equal to the saturation temperature corresponding to the measured pressure. Photographic, pressure, and wall-temperature data show that the liquid tended to cling to the container wall and move with it during spinning. The liquid mixed while the spin rate was changing.

The measured pressure was always greater than the computed thermal equilibrium pressure, which indicated that there was always subcooled liquid in the container. Much evidence, but no photographic proof, was accumulated to indicate that the liquid was always boiling for the average uniform heat-transfer rate of 132 Btu per hour per square foot. The heat-transport process within the liquid hydrogen may have been similar to subcooled nucleate boiling.

Lewis Research Center

National Aeronautics and Space Administration
Cleveland, Ohio, July 10, 1962

█



APPENDIX A

DETAILS OF ROCKET PERFORMANCE

Trajectory

The vertical trajectory determined by radar is compared with that predicted for the 303-pound payload and prevailing launch conditions in figure 15. This performance is normal and satisfactory.

Spin Rate

The spin-rate history determined by the sun sensors is shown in figure 16 and is conventional for this rocket until 120 seconds. At that time, pressurizing gas from the emptied fuel tank was discharged through a pair of nozzles mounted on the rocket just aft of the payload. The rocket despun almost as predicted, and the spin reached zero at 166 seconds. After 186 seconds, a malfunction in the turntable caused the experiment and the rocket to spin erratically until a complete electric failure occurred at 280 seconds. The system coasted to zero at 325 seconds just as the rocket began to spin again because of reentry into the atmosphere.


Attitude

The magnetometer data obtained are of questionable value probably because of flux interference from power sources in the payload. The longitudinal magnetometer output corrected for sudden changes of known cause is presented in figure 17. It can be concluded from these data that the vehicle did not undergo severe attitude changes.

Longitudinal Acceleration

The acceleration during the burning period is shown in figure 18(a). Peak acceleration (10.5 g) occurred near booster burnout; at sustainer burnout the acceleration was 7.5 g's.

The acceleration after burnout due to the net effect of drag and ant drag thrust is shown in figures 18(b) and (c). The liquid-hydrogen container wall-temperature data show that the accelerometer output should have been more nearly the dot-dash curve of figure 18(c) up to 56 seconds. Both thrust and drag approached zero after 100 seconds. Later, when the experiment (in which the accelerometers were mounted) spun the accelerometer output was oscillatory with the average value greater than zero. Such output shows that the instrument was neither on the true spin axis nor parallel to it.





DECLASSIFIED

APPENDIX B

LIQUID-HYDROGEN CONTAINER WALL TEMPERATURE

Curves were faired through raw data from each wall-temperature transducer. More than 90 percent of the individual data points were scattered less than 2° R from the faired curves. The changes in temperature read from these curves were consistent among adjacent transducers, but levels differed by 2° to 8° R. In order to get a better representation of the true temperature, a correction based on the following assumptions was applied to the data from each transducer:

(1) Just after the liquid hydrogen had splashed the top of the sphere, the heat-transfer rate to the hydrogen was negligible because the heaters were still cool.

(2) At the same time, the hydrogen became well mixed and washed the whole inside surface of the container; therefore, each transducer should read very close to existing saturation temperature.

The wall-temperature data corrected in this manner are presented in figure 19. It is felt that the method of correction does not destroy the accuracy of the changes in temperature, and, thus, the data shown are accurate to about $\pm 2^{\circ}$ R.



031712201030

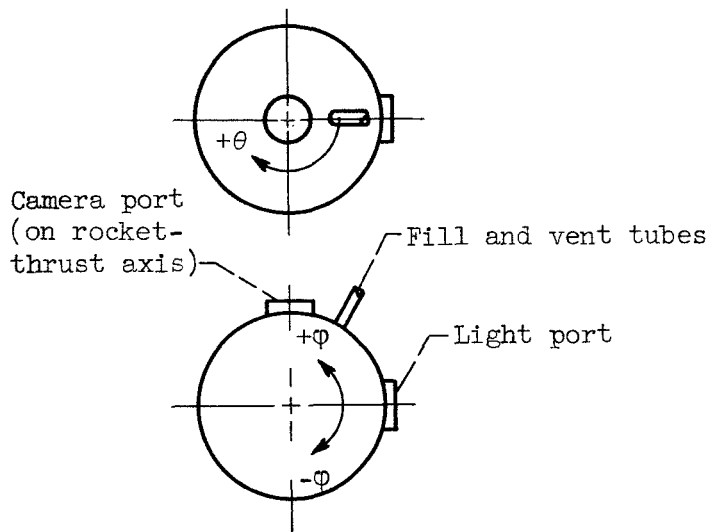


REFERENCES

1. Benedikt, E. T.: General Behavior of a Liquid in a Zero or Near Zero Gravity Environment. Astro Sciences Group Rep. ASG-TM-60-9Z6, Norair Div., Northrop Corp., May 1960.
2. Li, Ta: Liquid Behavior in a Zero-G Field. Rep. AE-60-0682, Convair Astronautics, Aug. 1960.
3. Li, Ta: Cryogenic Liquids in the Absence of Gravity. Paper presented at 1961 Cryogenic Eng. Conf., Ann Arbor (Mich.), Aug. 1961.
4. Petrash, Donald A., Zappa, Robert F., and Otto, Edward W.: Experimental Study of the Effects of Weightlessness on the Configuration of Mercury and Alcohol in Spherical Tanks. NASA TN D-1197, 1962.
5. Reynolds, W. C.: Hydrodynamic Considerations for the Design of Systems for Very Low Gravity Environments. Tech. Rep. LG-1, Thermosci. Div., Dept. Mech. Eng., Stanford Univ., Sept. 1961.
6. Usiskin, C. M., and Siegel, R.: An Experimental Study of Boiling in Reduced and Zero Gravity Fields. Paper 60-HT-10, ASME-AIChE, 1960.
7. Steinle, H. F., and Schwartz, E. W.: An Experimental Study of the Transition from Nucleate to Film Boiling Under Zero Gravity Conditions. Rep. AZJ-55-009, Convair Astronautics, Nov. 23, 1959.
8. Knoll, Richard H., Smolak, George R., and Nunamaker, Robert R.: Weightlessness Experiments with Liquid Hydrogen in Aerobee Sounding Rockets; Uniform Radiant Heat Addition - Flight 1. NASA TM X-484, 1962.
9. Goodwin, R. D., et al.: Provisional Thermodynamic Functions for Para Hydrogen. Rep. 6791, NBS, Aug. 4, 1961.
10. Aerophysics Group: June-August Progress Report for the Combined Laboratory and KC-135 Aircraft Zero-G Test Program. Rep. AE61-0871, Convair Astronautics, Sept. 5, 1961.



TABLE I. - SPHERICAL COORDINATES FOR TEMPERATURE
TRANSDUCERS ON LIQUID-HYDROGEN SPHERE



Transducer	ϕ , deg	θ , deg
2	-15	172
3	-32	240
4	-73	330
5	-43	111
6	5	129
7	13	218
8	-28	298
9	-37	46
10	6	78
11	44	172
13	-16	354
14	19	28
17	24	328
18	64	340
19	54	28
20	40	54
21	24	68
22	-16	90
23	-27	97



037122030

TABLE II. - FLIGHT SYNOPSIS FOR NASA

AEROBEE 4.39 [PAYLOAD, 303 LB.]

Altitude, ft	Time from liftoff, sec	Event
58,000	40	Camera on; heater on
106,000	52.5	Burnout; antidrag nozzle open
369,000	120	Despin nozzles open
467,000	166	Despin completed
491,000	186	Experiment starts spinning
499,000	199	Experiment stops spinning
502,000	212	Experiment starts spinning
503,000	214	Apogee (95 stat. miles)
358,000	310	Collection nozzles open
306,000	326	Experiment stops spinning
215,000	350	Camera package separates

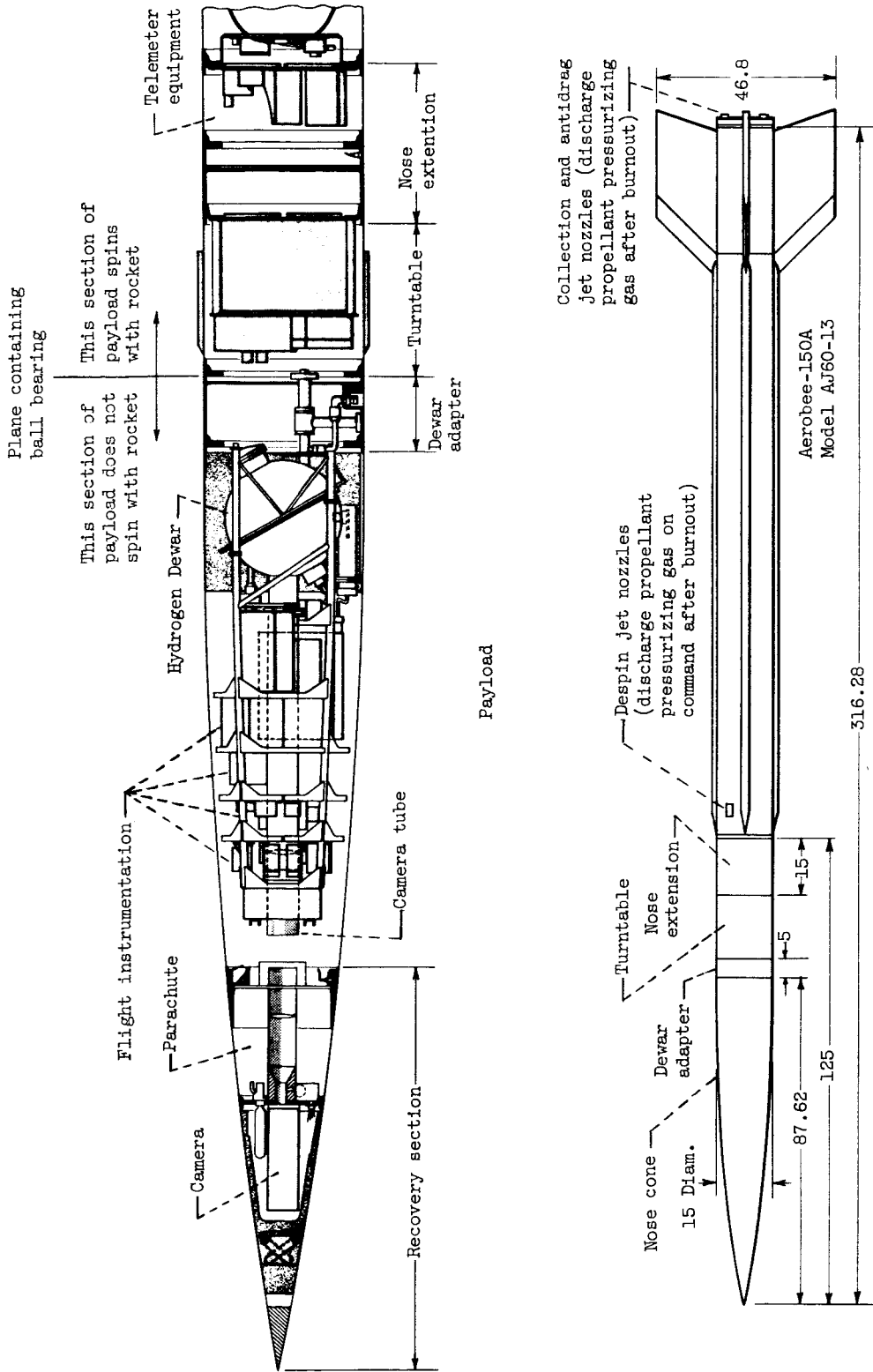


Figure 1. - Sketch of rocket and payload. (Dimensions in inches.)

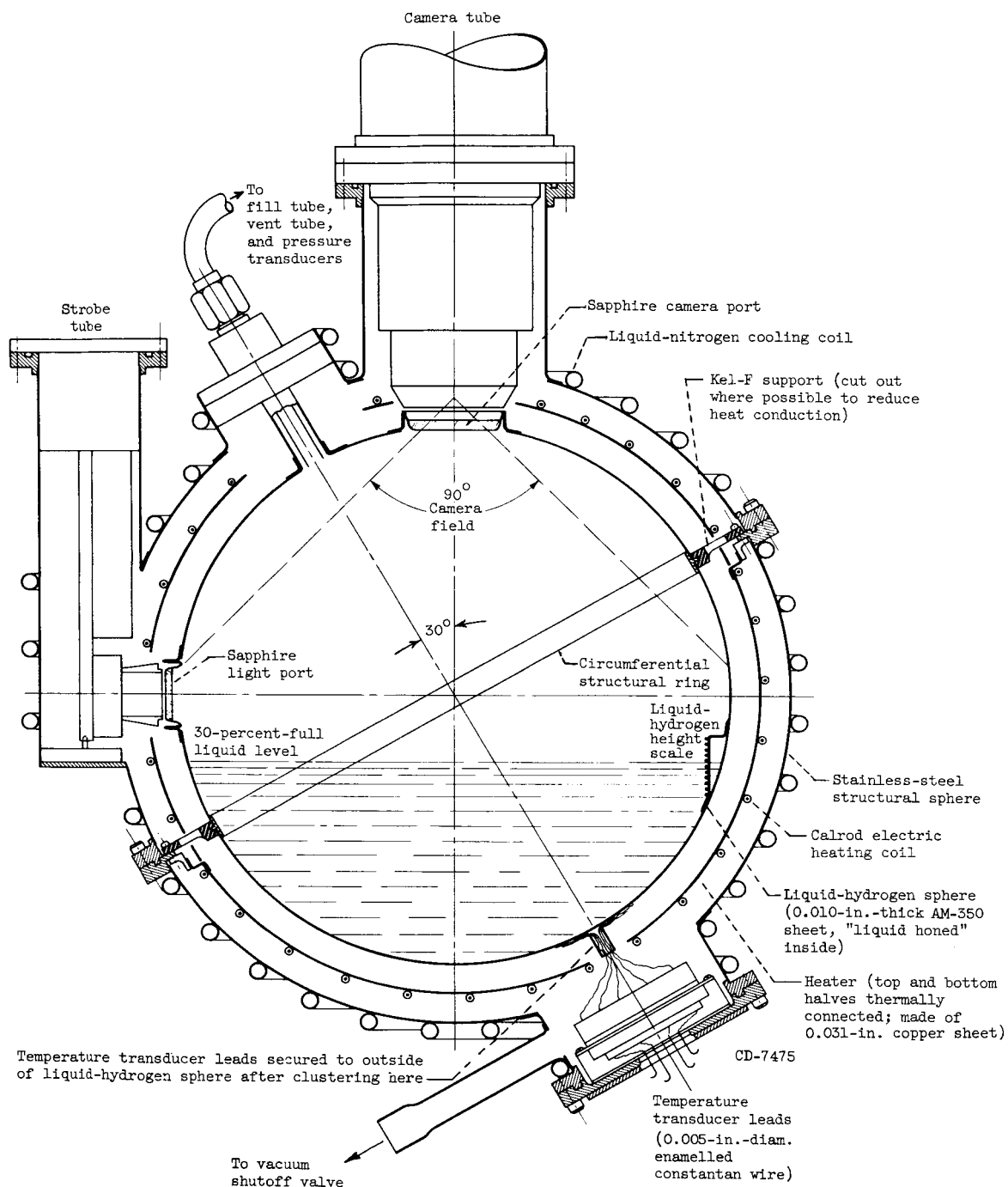


Figure 2. - Schematic of 9-inch-diameter spherical liquid-hydrogen Dewar.



SECRET

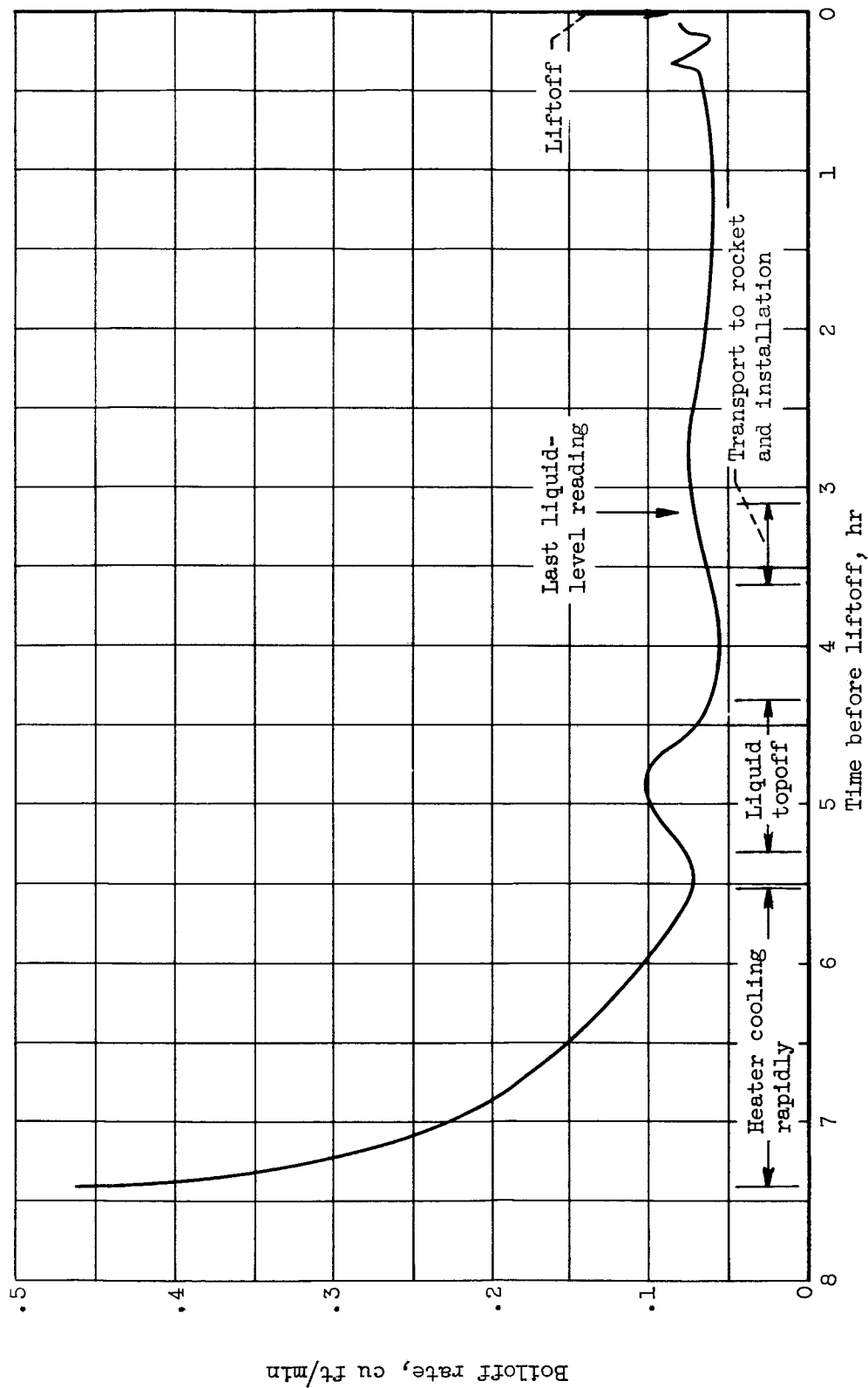


Figure 3. - Prelaunch liquid-hydrogen boiloff measured at approximately standard pressure and temperature. Experiment vented to atmosphere through gas meter.

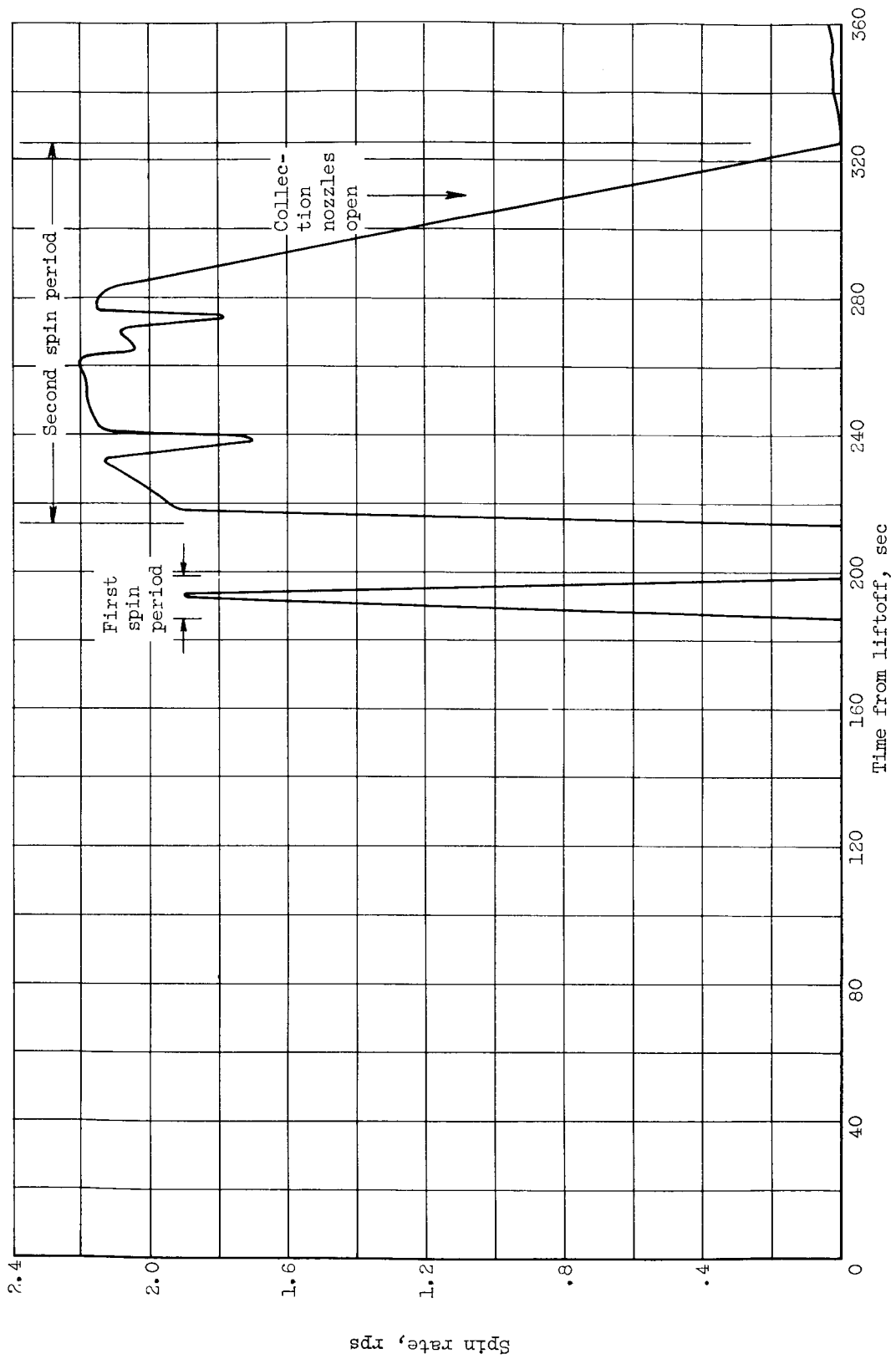


Figure 4. - Experiment spin rate. Experiment spins counterclockwise as vehicle comes toward viewer.

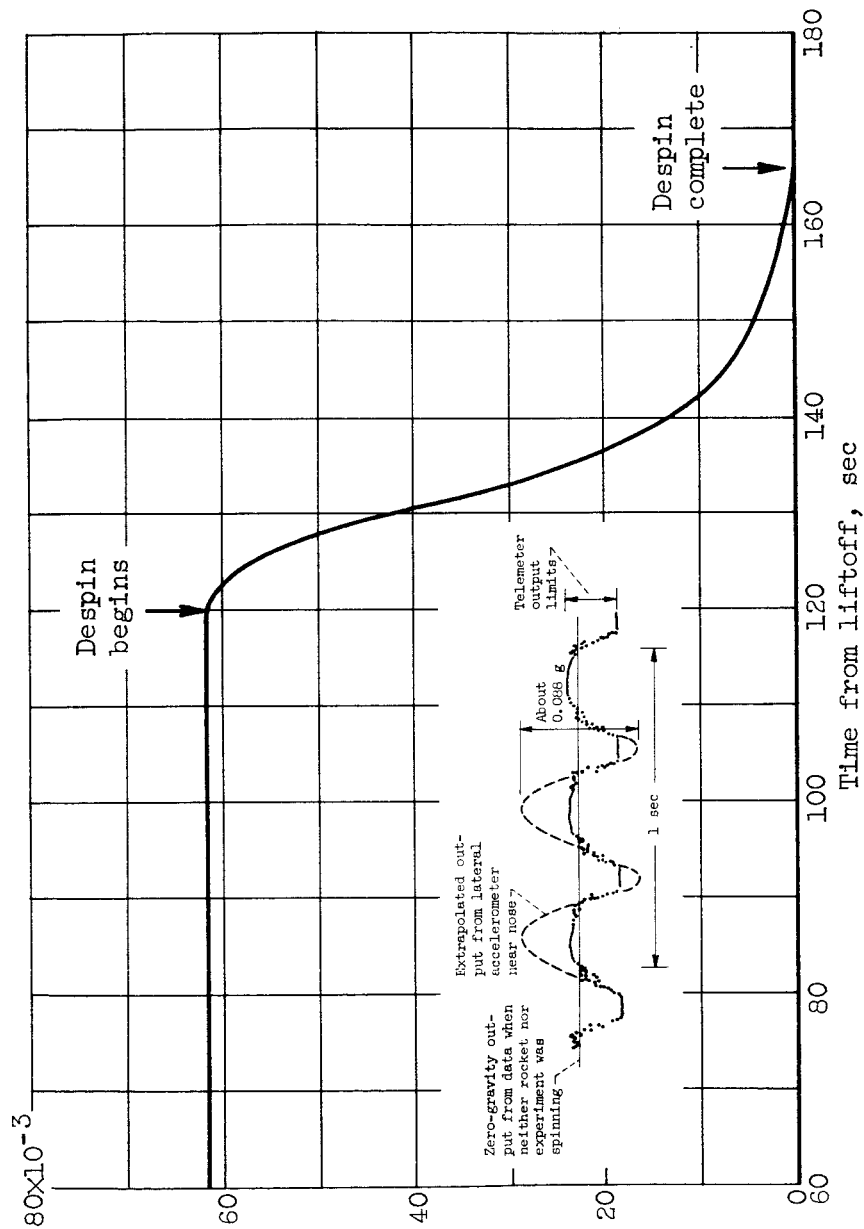


Figure 5. - Lateral acceleration at liquid-hydrogen Dewar during despin period.

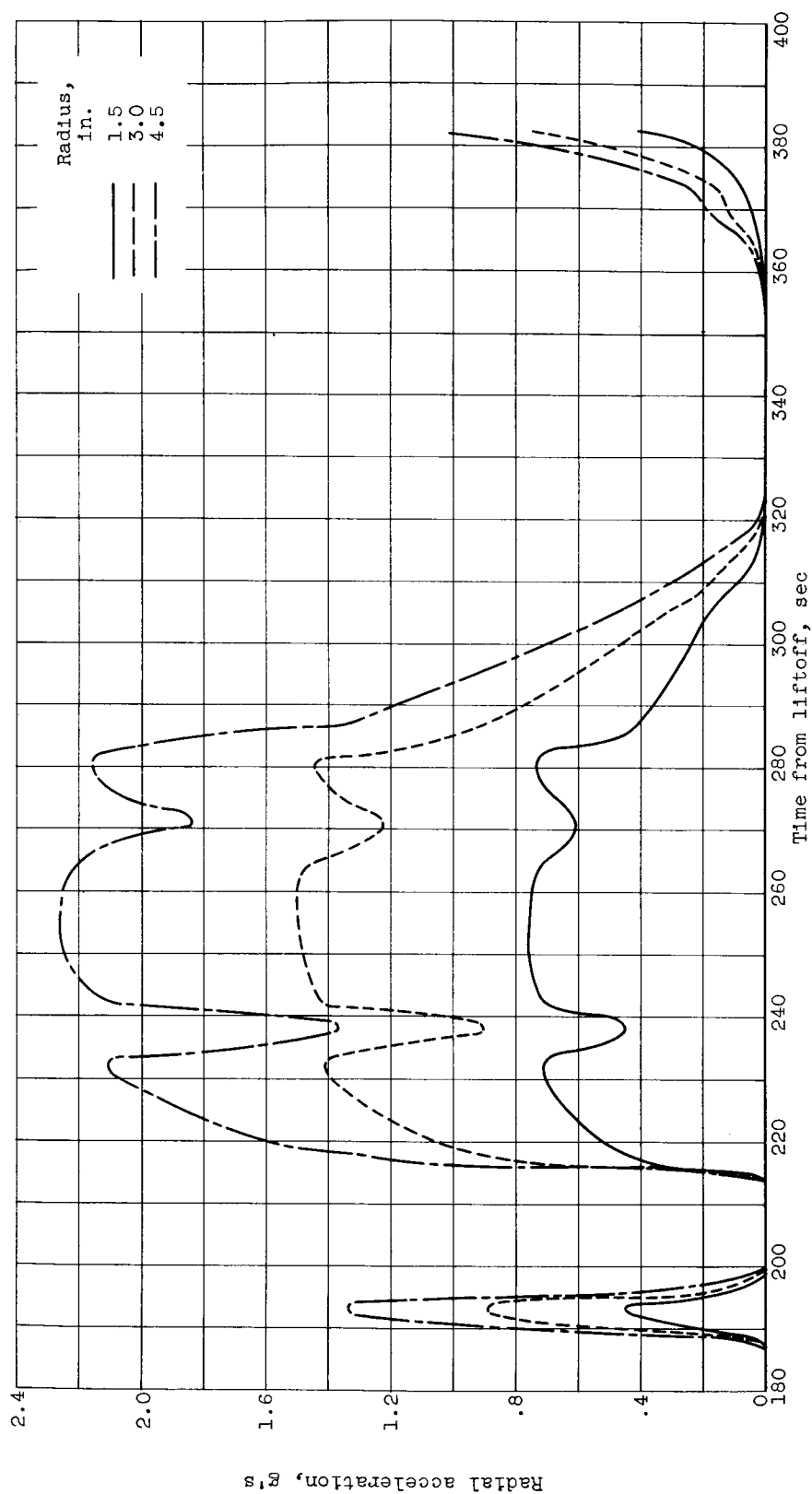
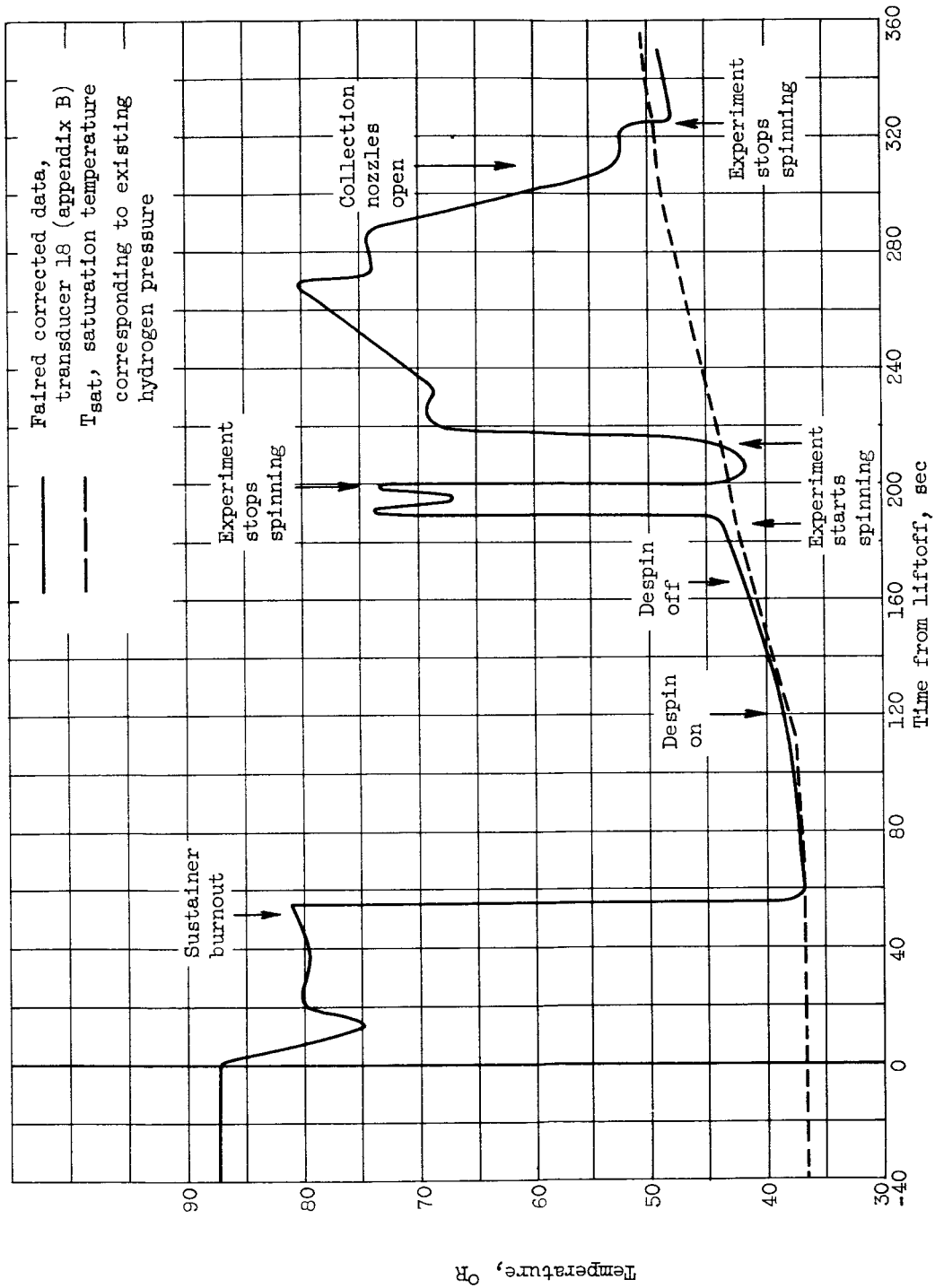
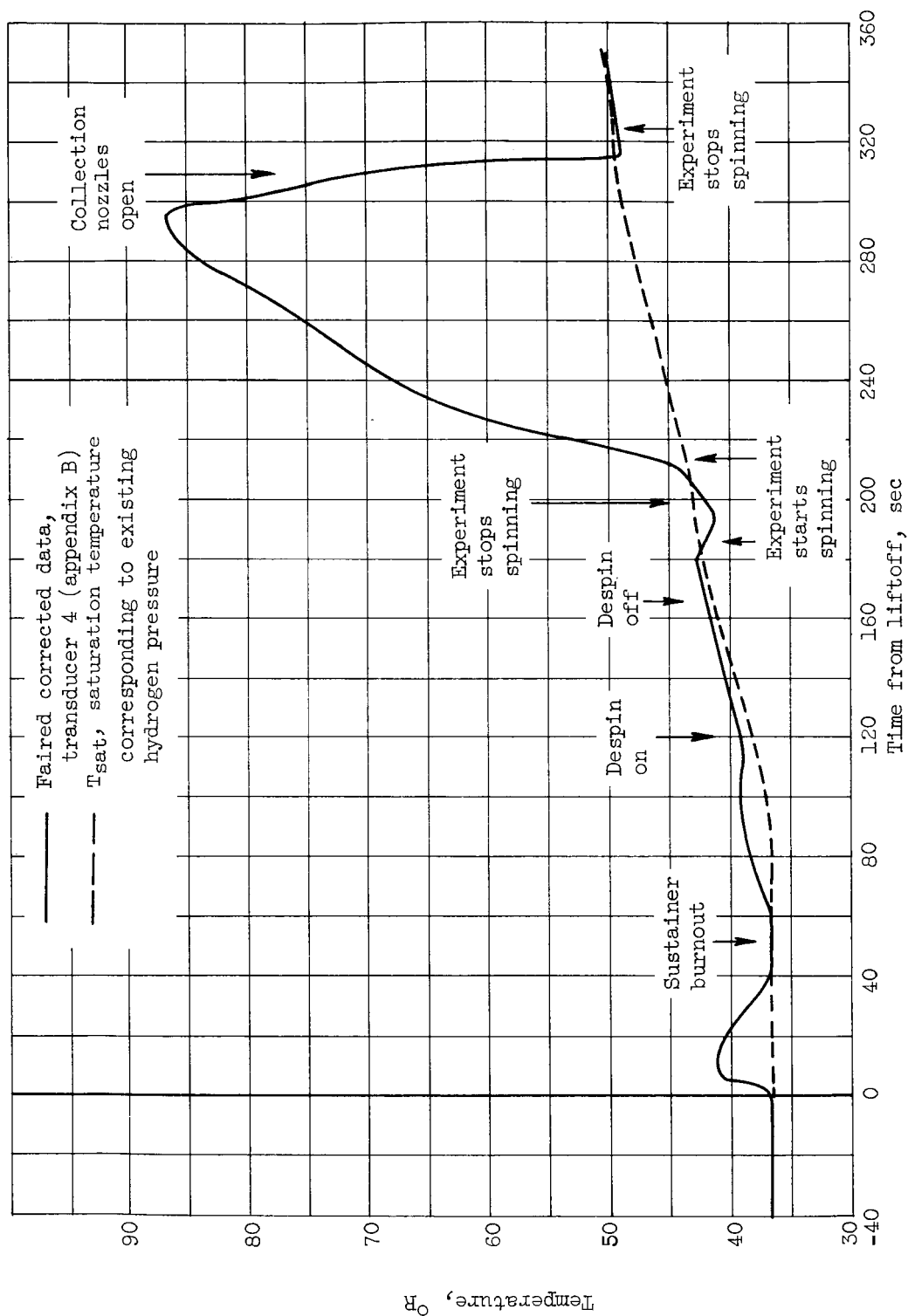


Figure 6. - Radial acceleration caused by experiment spin only, for particles at radii of 1.5, 3.0, and 4.5 inches.



(a) Near spin axis, top.

Figure 7. - Typical liquid-hydrogen sphere-wall temperature histories.

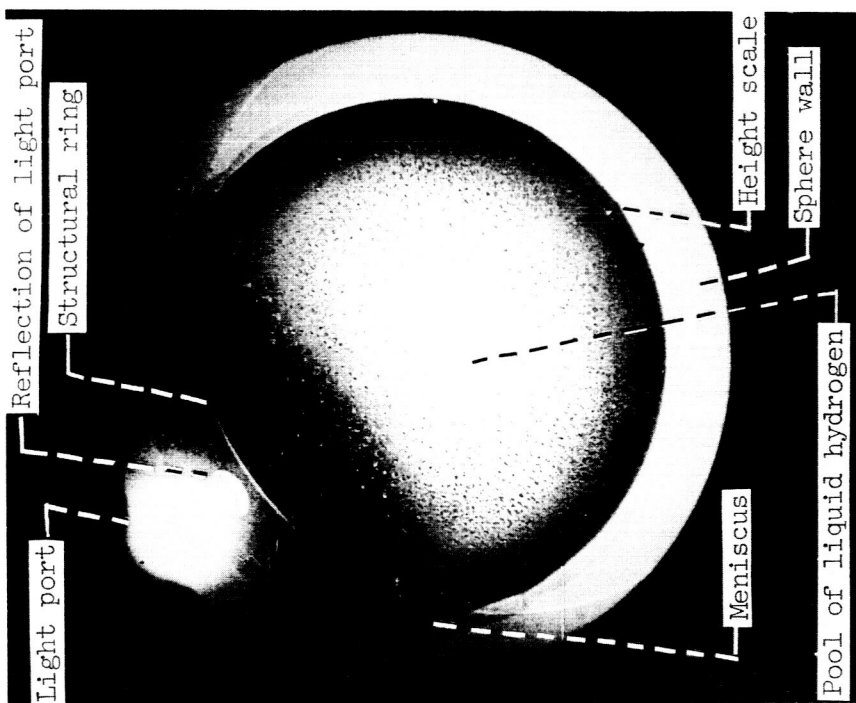


(b) Near spin axis, bottom.

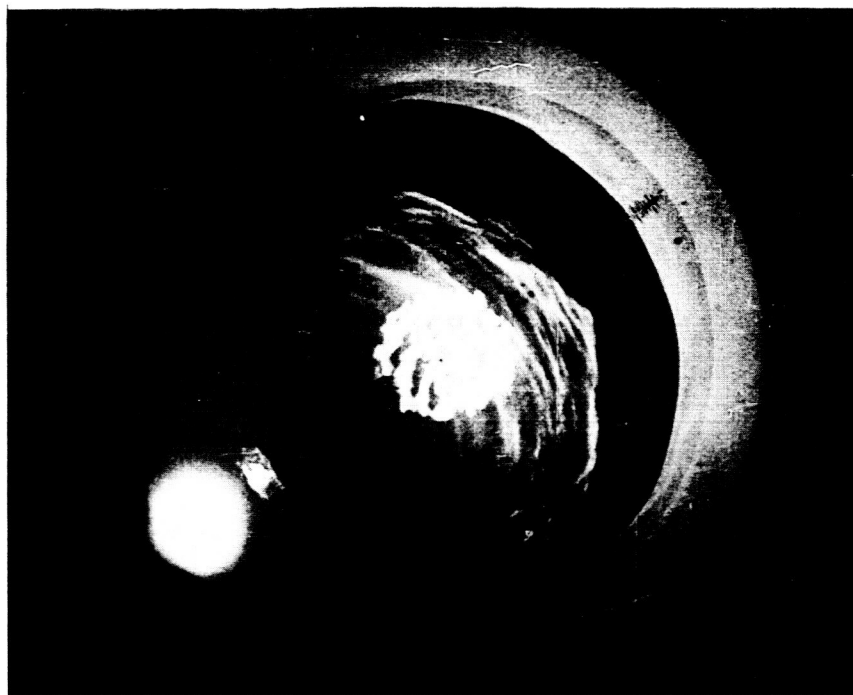
Figure 7. - Concluded. Typical liquid-hydrogen sphere-wall temperature histories.



CONFIDENTIAL



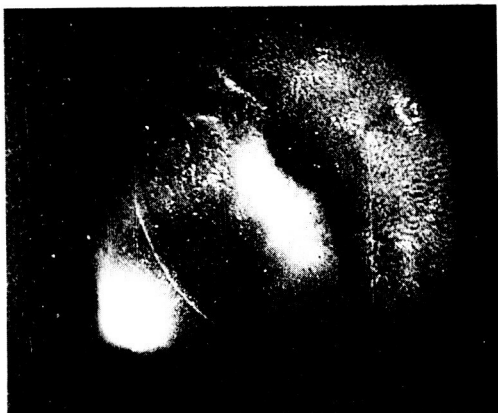
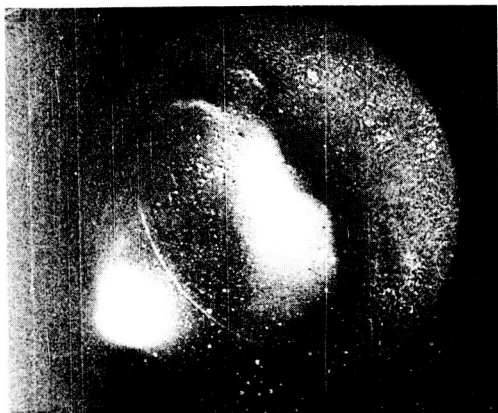
(a) Prior to launch.



C-61081

(b) During sustainer burning.

Figure 8. - Inside of liquid-hydrogen Dewar.



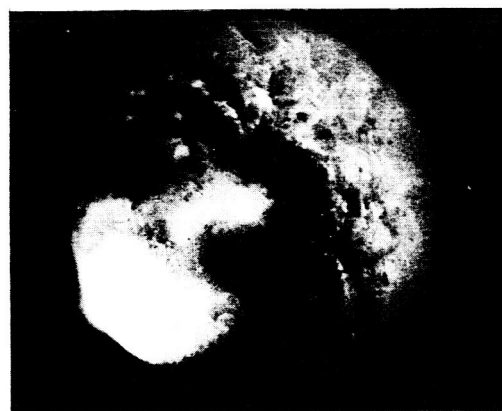
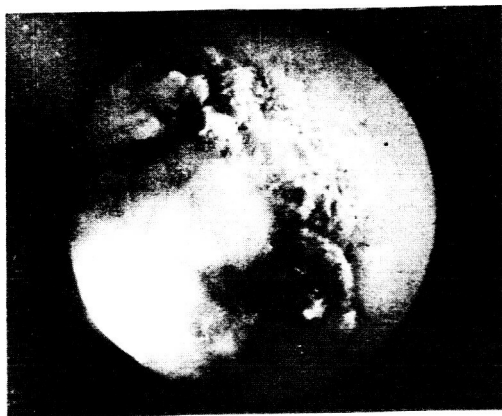
C-61082

Time →

(c) 80 seconds after liftoff; exposure interval, approximately 0.2 second.
Figure 8. - Continued. Inside of liquid-hydrogen Dewar.



DECLASSIFIED



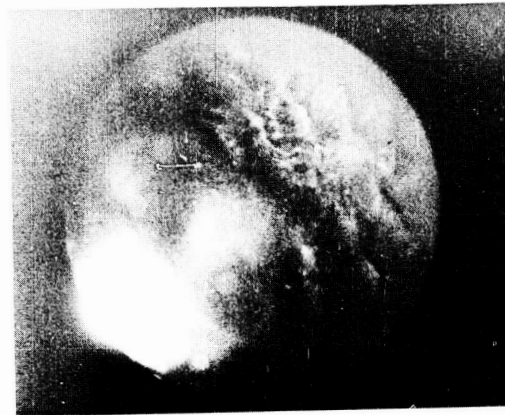
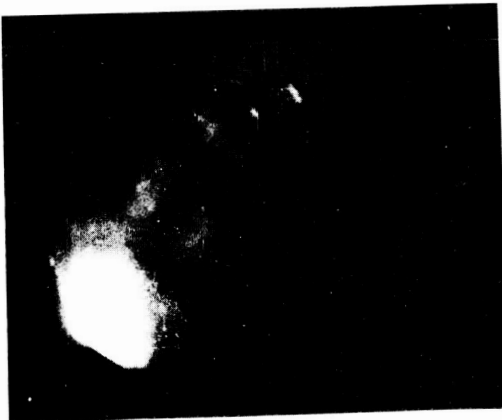
C-61083

Time →

(d) 110 seconds after liftoff; exposure interval, approximately 0.2 second.

Figure 3. - Continued. Inside of liquid-hydrogen Dewar.

0371220030



C-61084

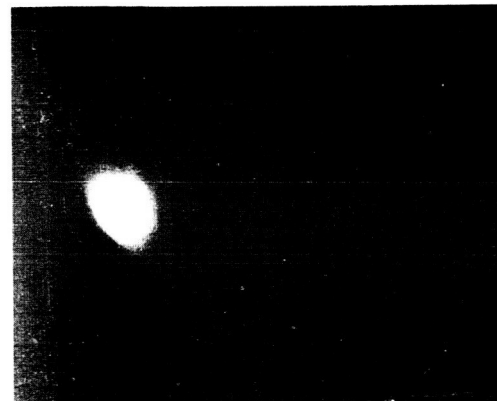
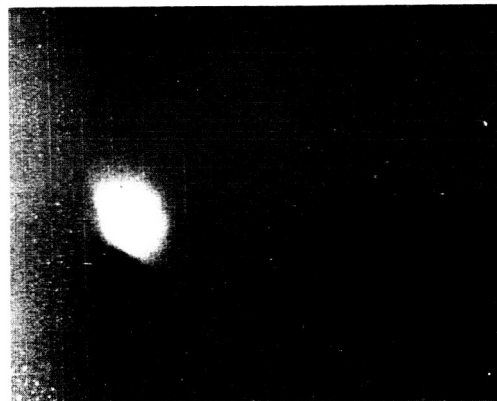
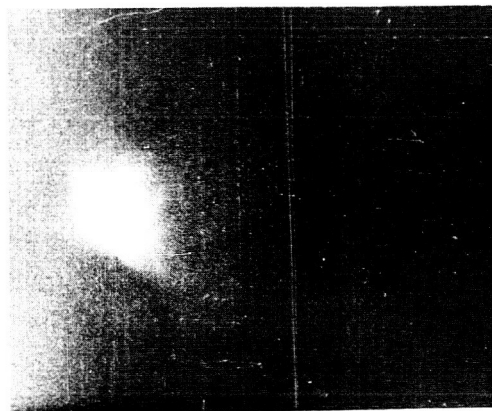
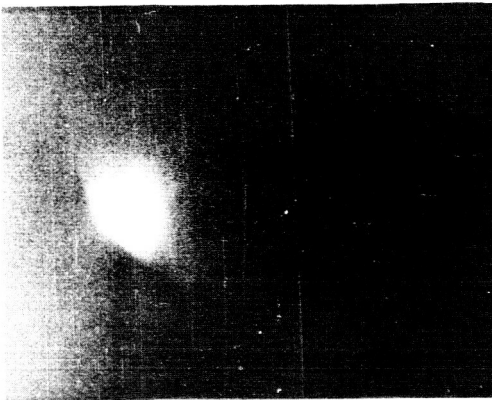
Time →

(e) 116 seconds after liftoff; exposure interval, approximately 0.2 second.

Figure 8. - Continued. Inside of liquid-hydrogen Dewar.



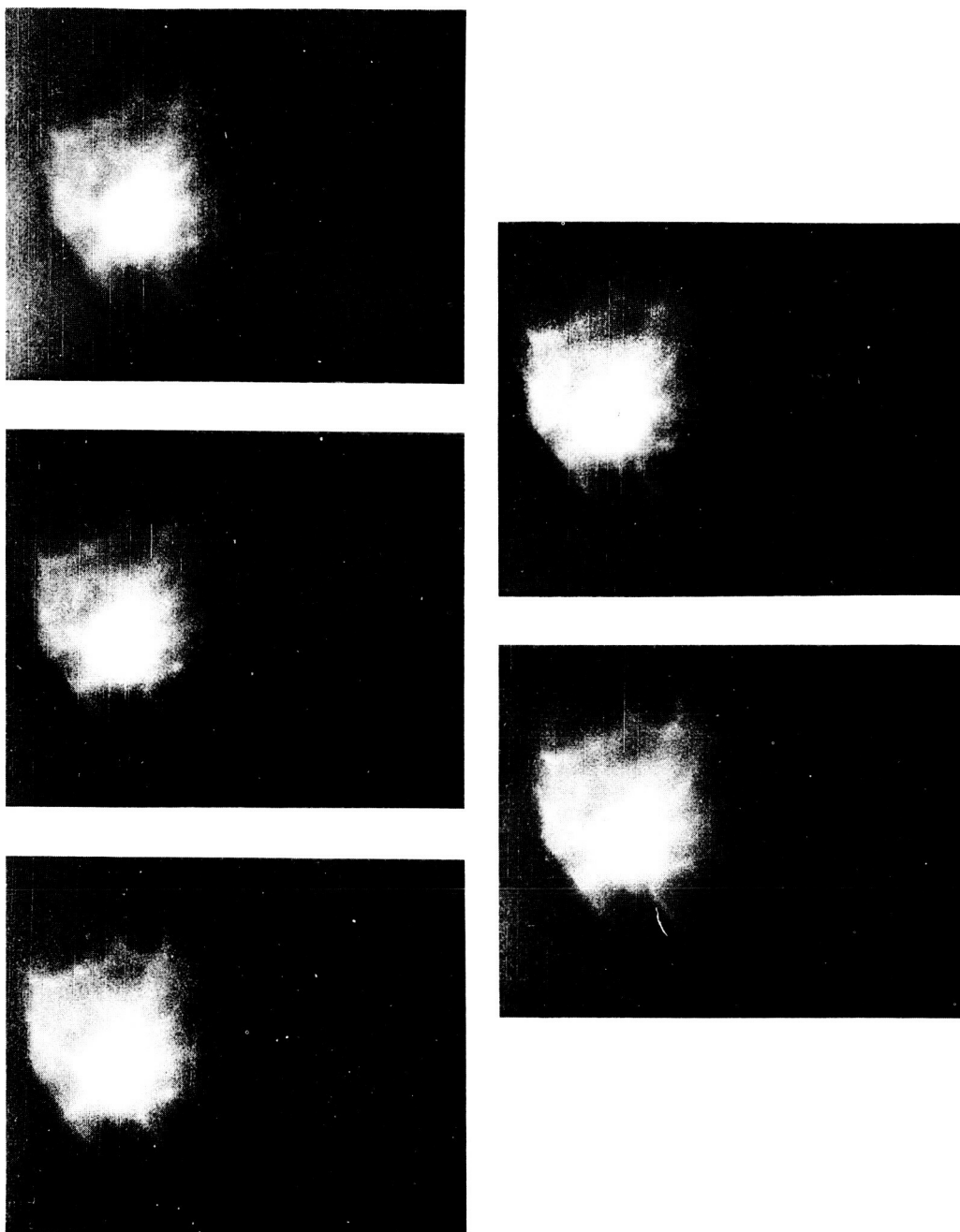
DECLASSIFIED



Time → C-61085
(r) 138 seconds after liftoff; exposure interval, approximately 0.2 second.
Figure 8. - Continued. Inside of liquid-hydrogen Dewar.

0371000000

00



C-61086

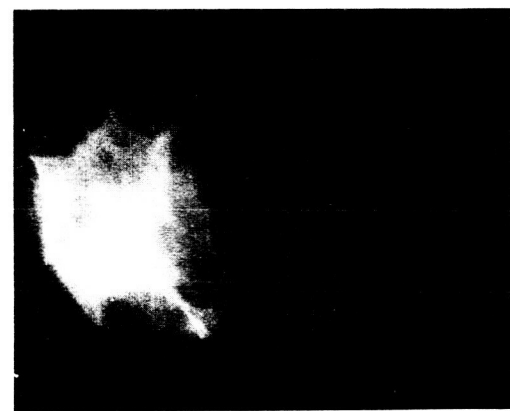
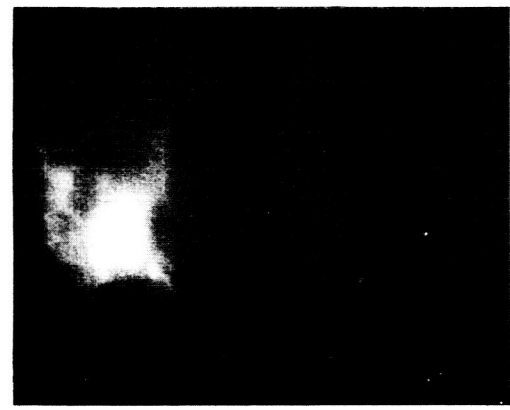
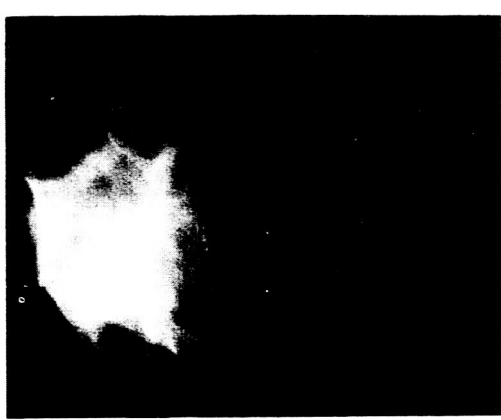
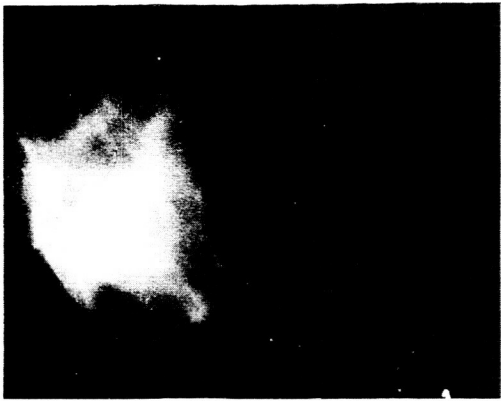
Time →

(E) 171 seconds after liftoff; exposure interval, approximately 0.2 second.

Figure 8. - Continued. Inside of liquid-hydrogen Dewar.



DECLASSIFIED



C-61087

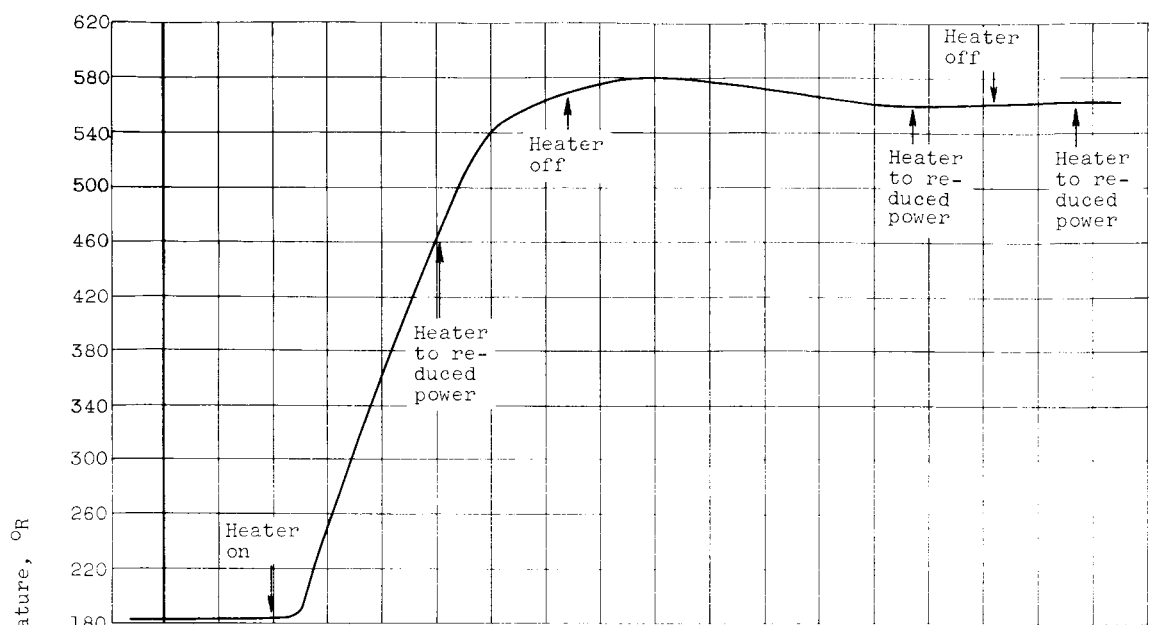
Time →

(h) 180 seconds after liftoff; exposure interval, approximately 0.2 second.

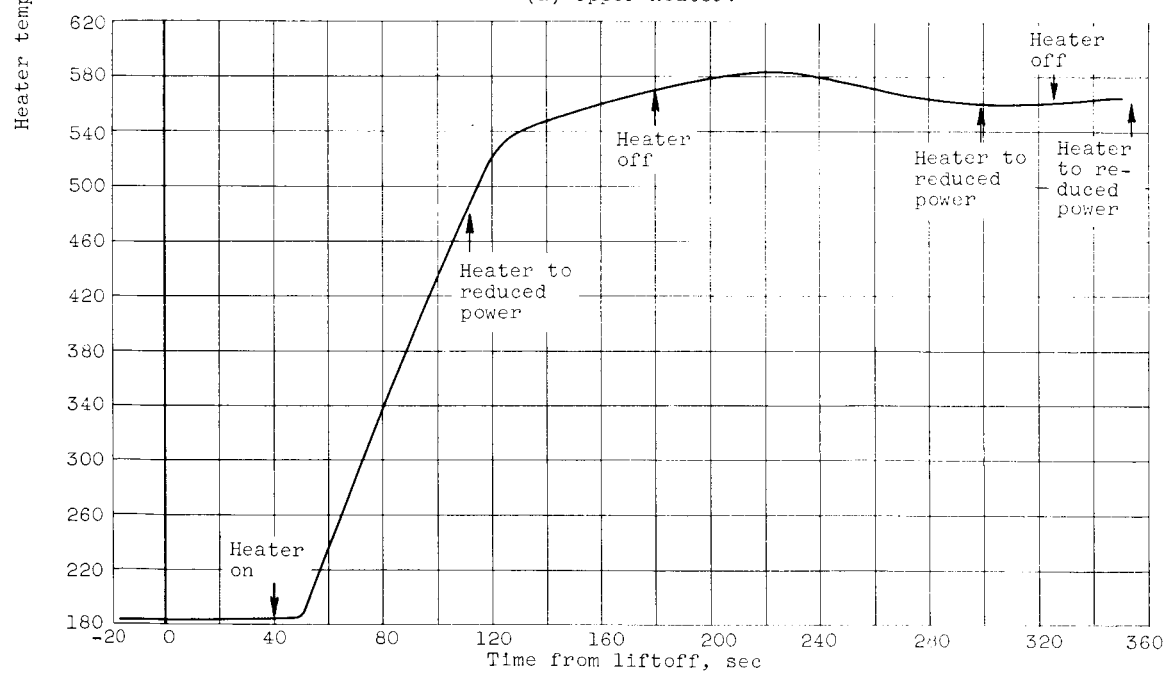
Figure 9. - Concluded. Inside of liquid-hydrogen vapor.

037125030

03

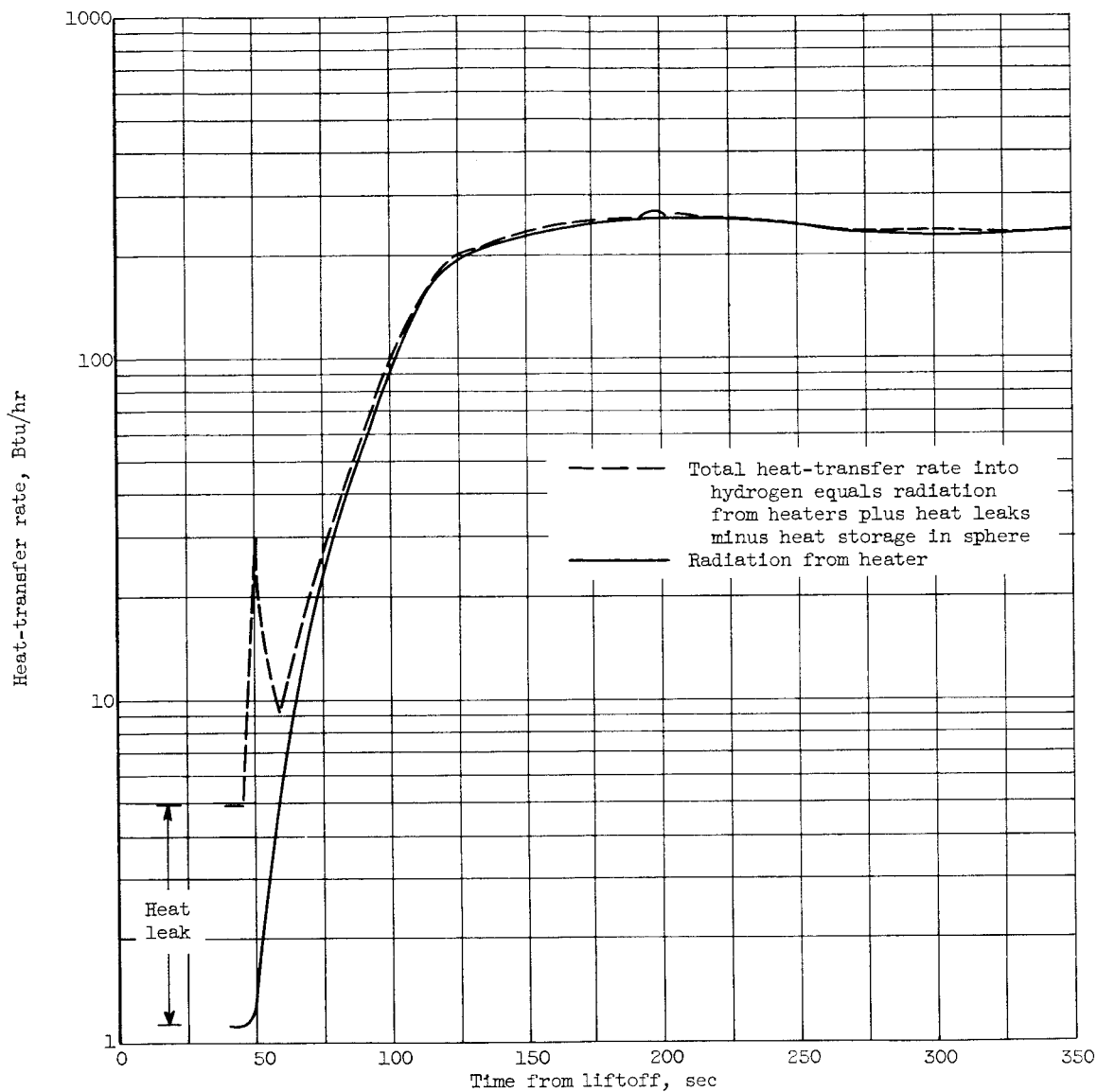


(a) Upper heater.



(b) Lower heater.

Figure 9. - Heater temperature history.

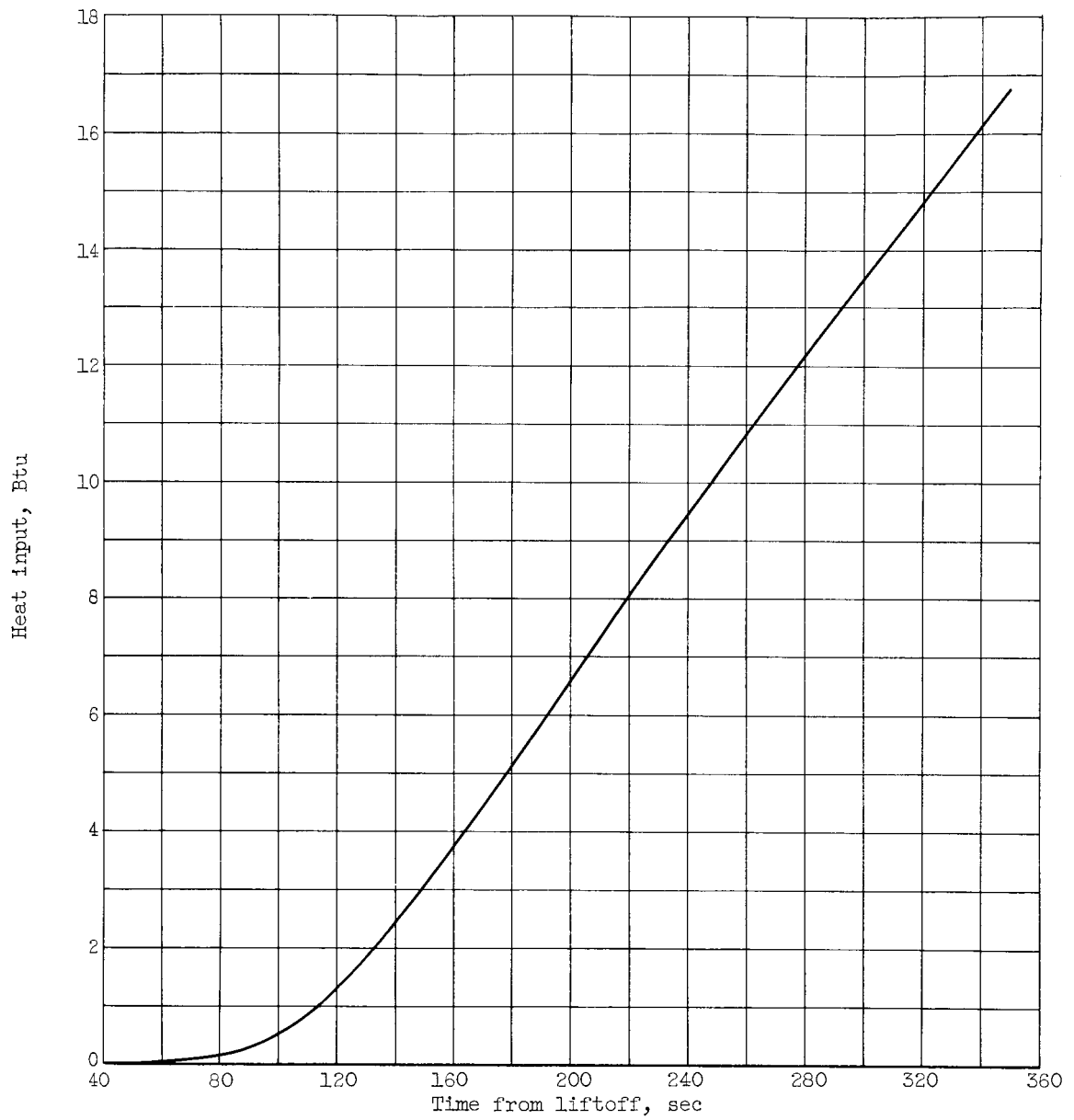


(a) Heat-transfer-rate history.

Figure 10. - Heat transferred to hydrogen.

CONFIDENTIAL

34



(b) Heat-input history.

Figure 10. - Concluded. Heat transferred to hydrogen.

CONFIDENTIAL

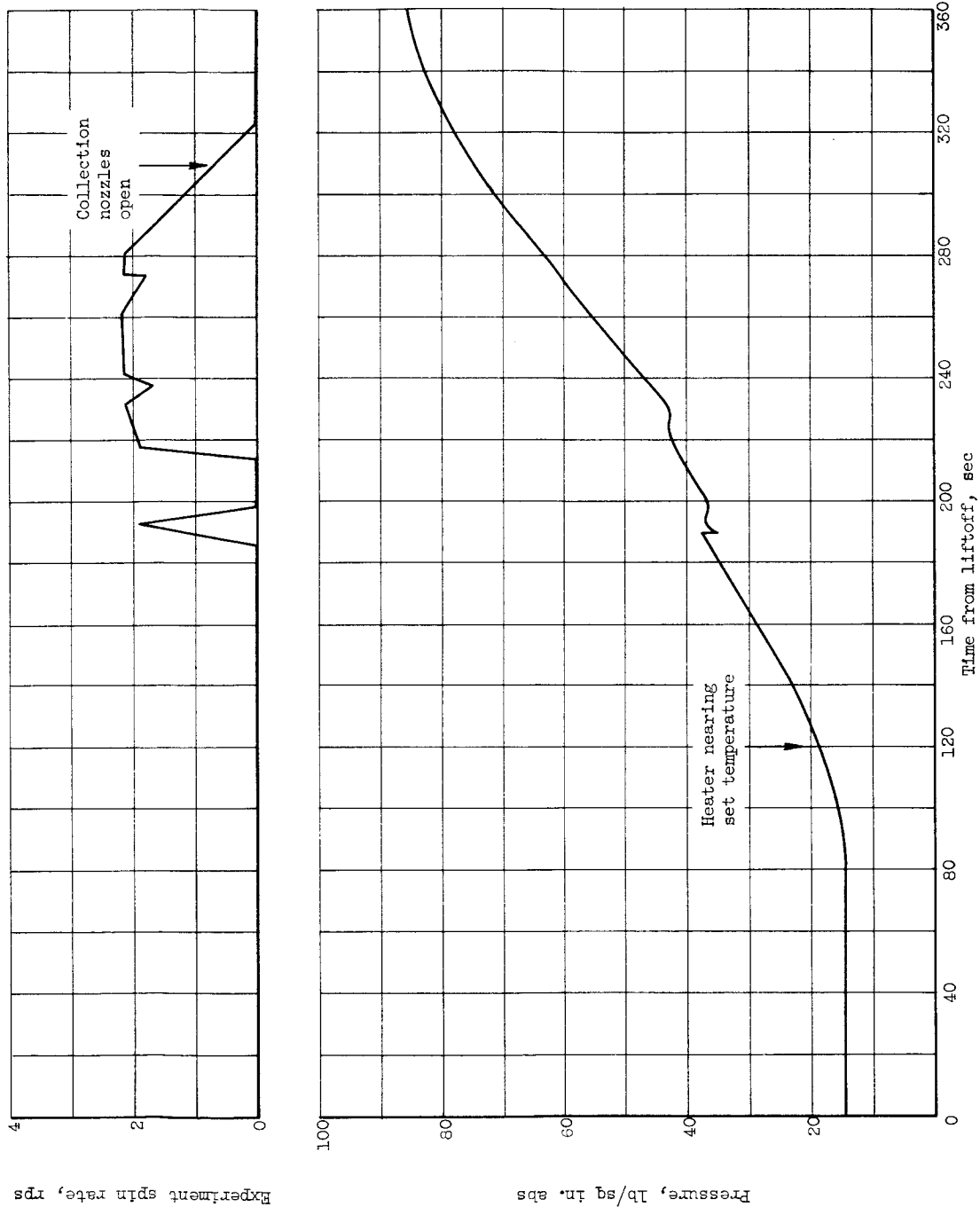


Figure 11. - Hydrogen-pressure history.

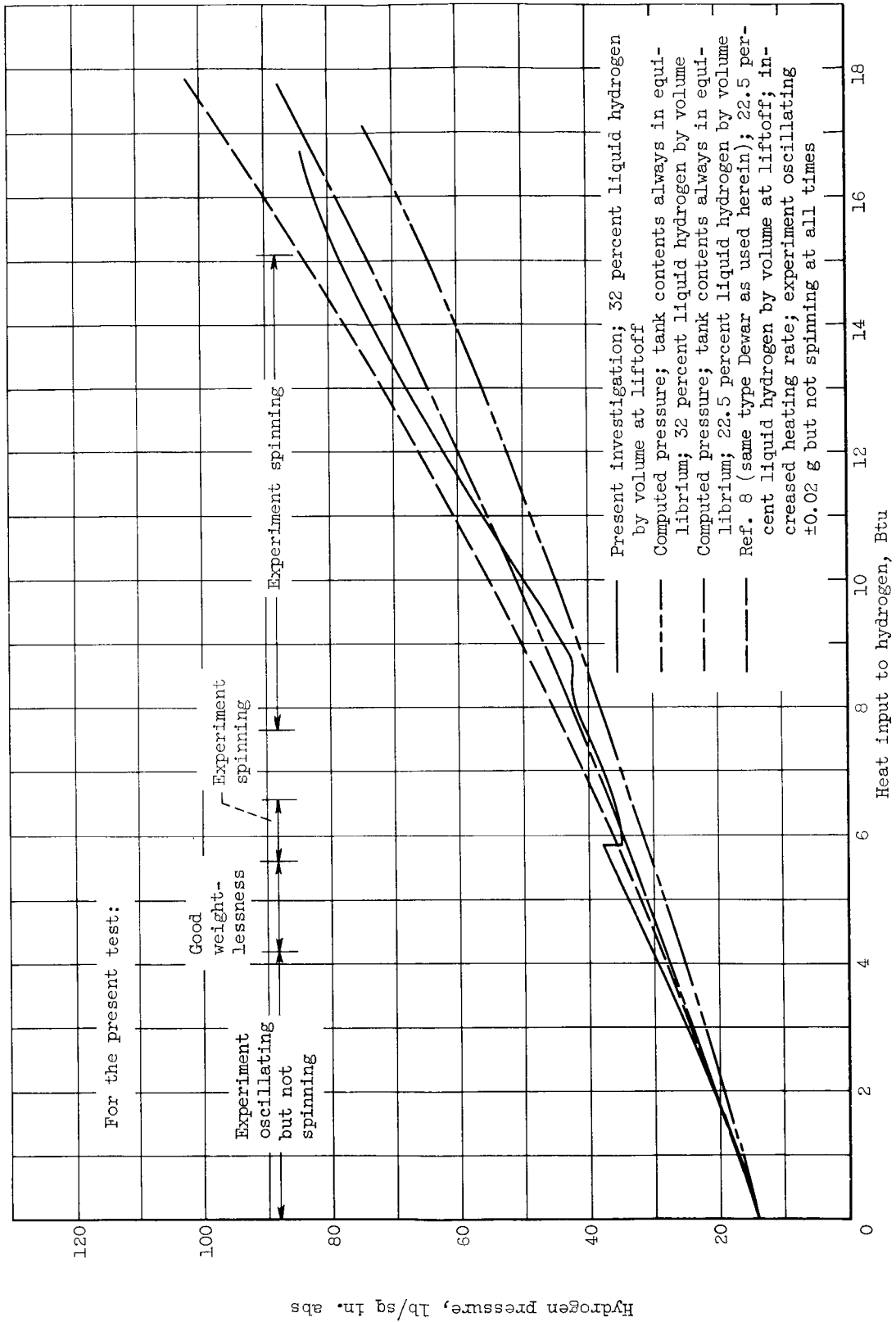


Figure 12. - Comparison of pressure rise in similar liquid-hydrogen containers for flight tests.

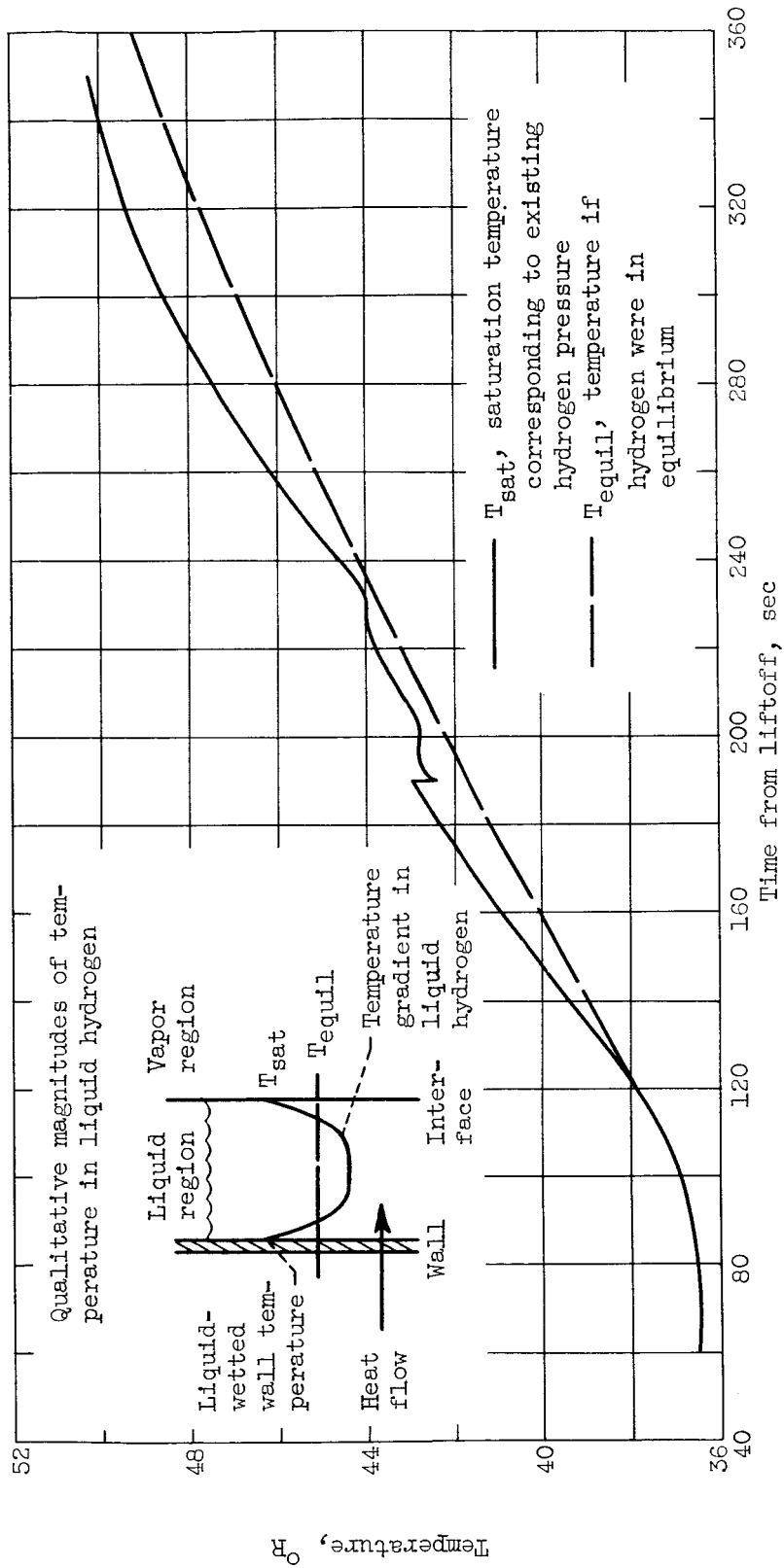


Figure 13. - Comparison of saturation and equilibrium temperatures.

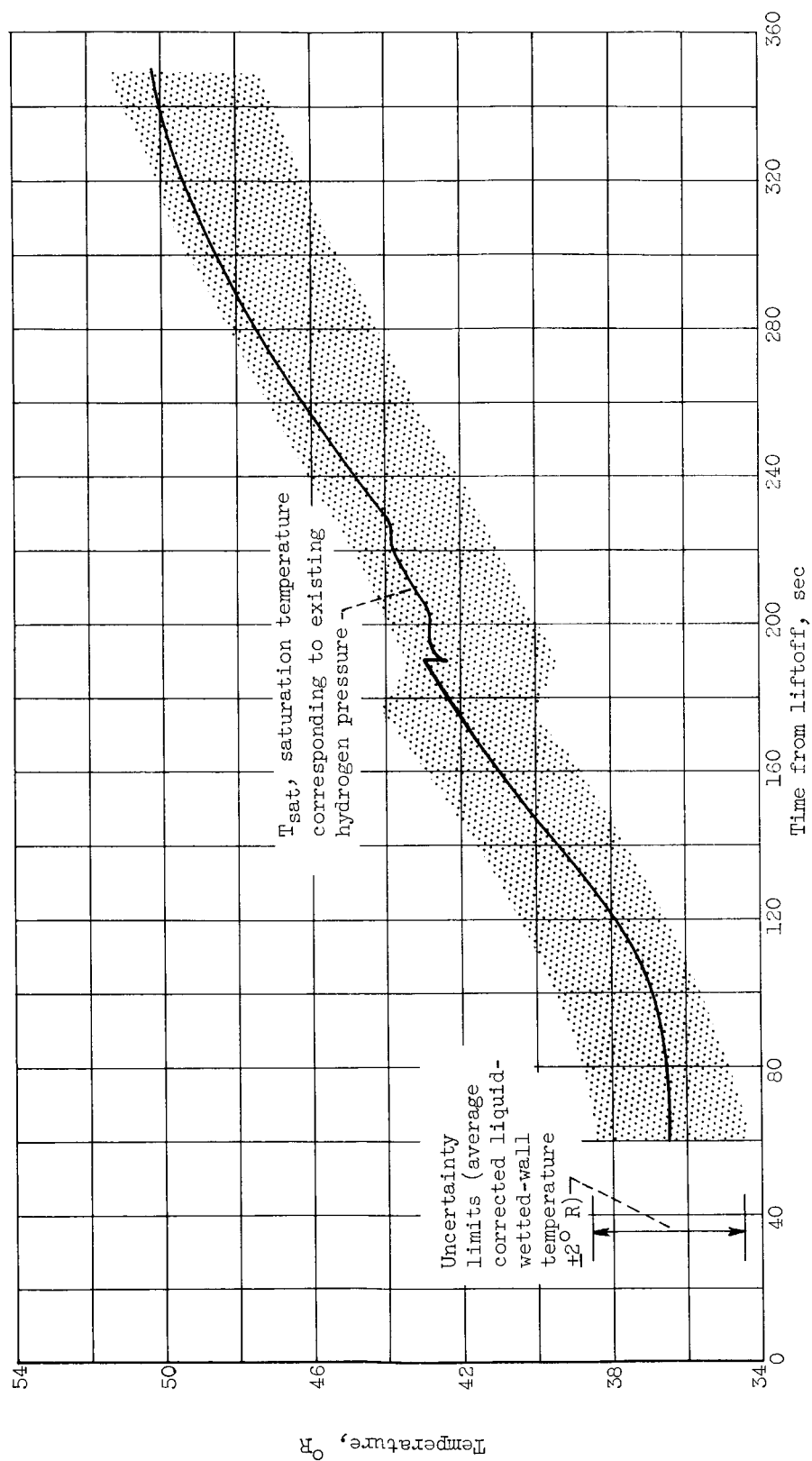


Figure 14. - Comparison of average liquid-wetted-wall temperature with saturation temperature.

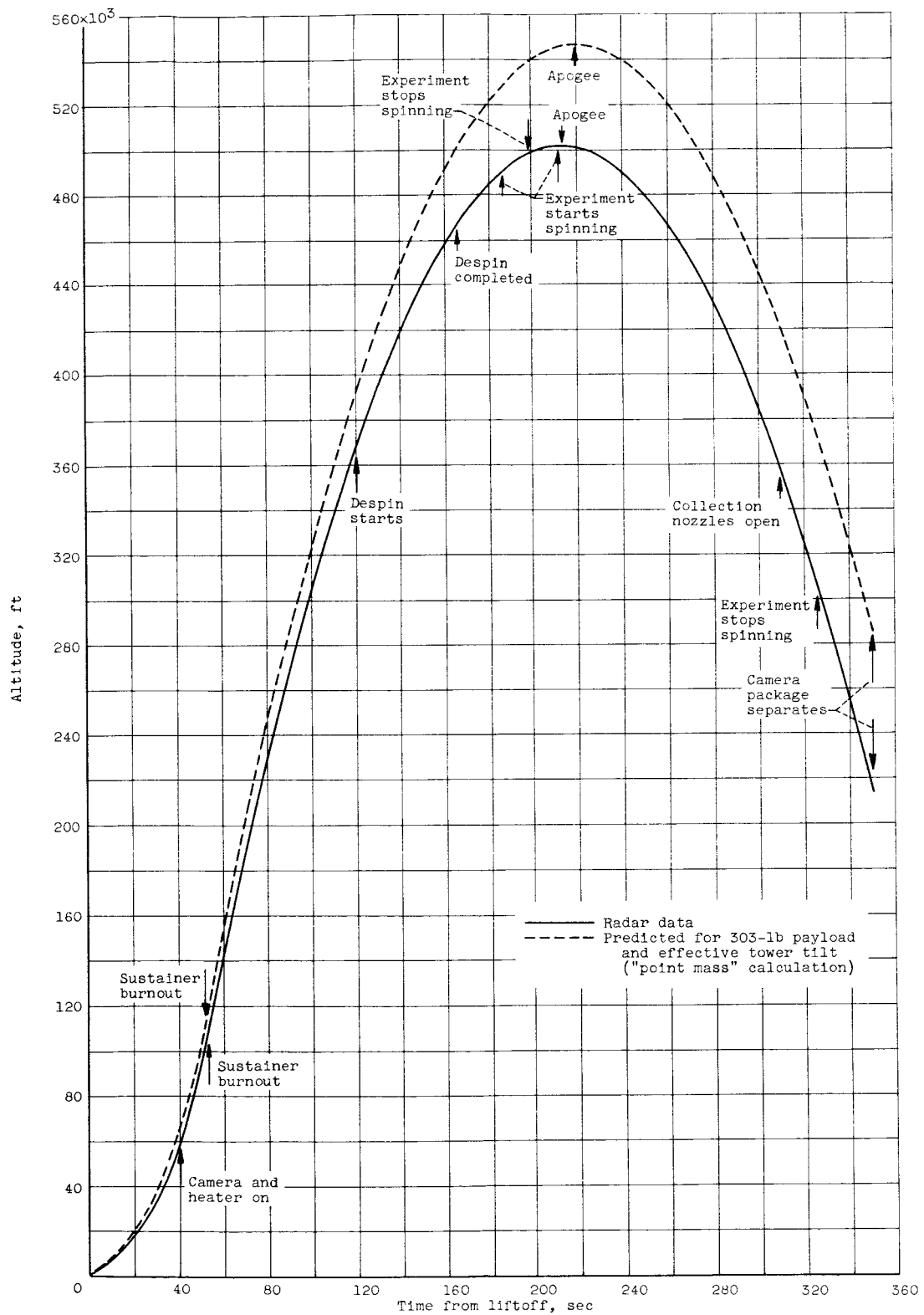


Figure 15. - Vertical trajectory of rocket.



03712 [REDACTED]

[REDACTED]

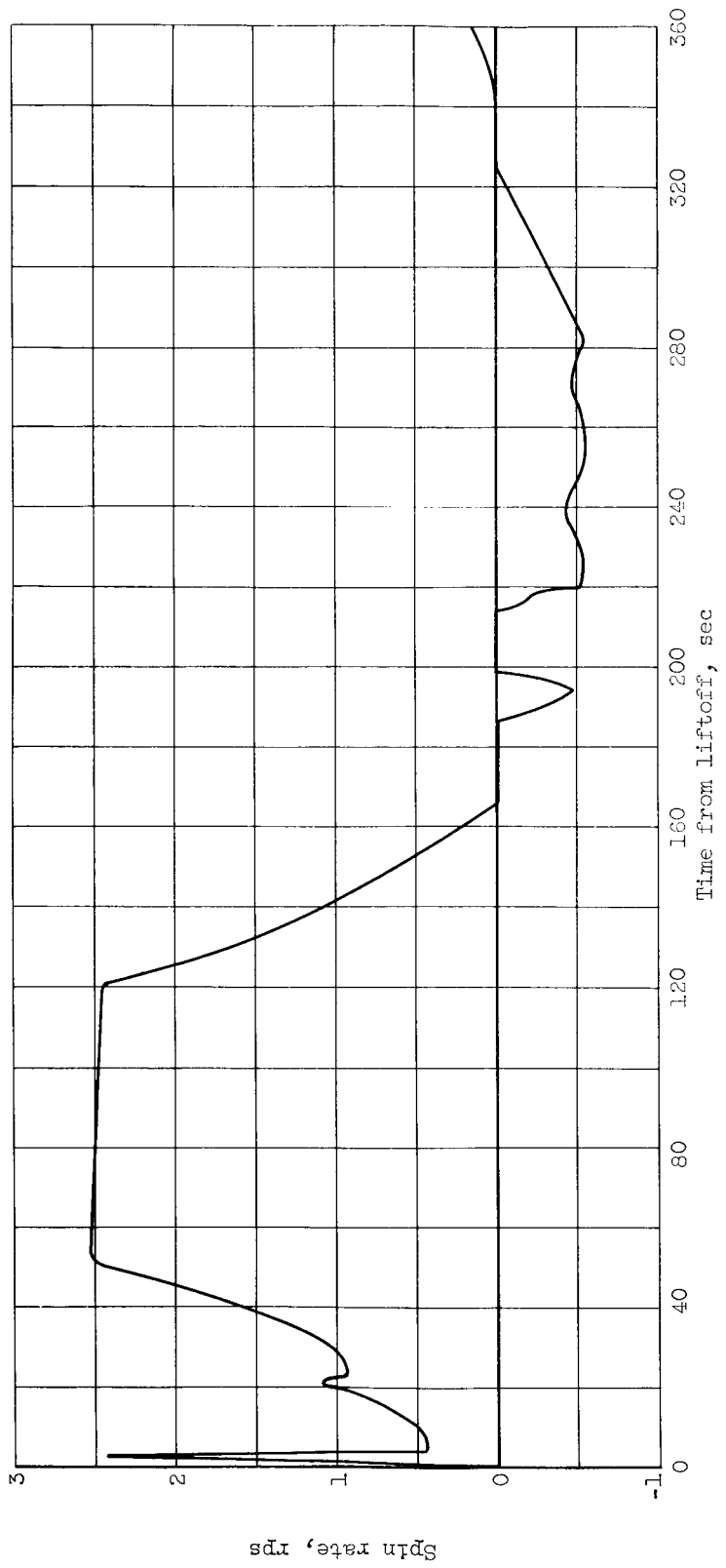


Figure 16. - Rocket spin-rate history. Spin is positive for counterclockwise rotation as rocket comes toward viewer.

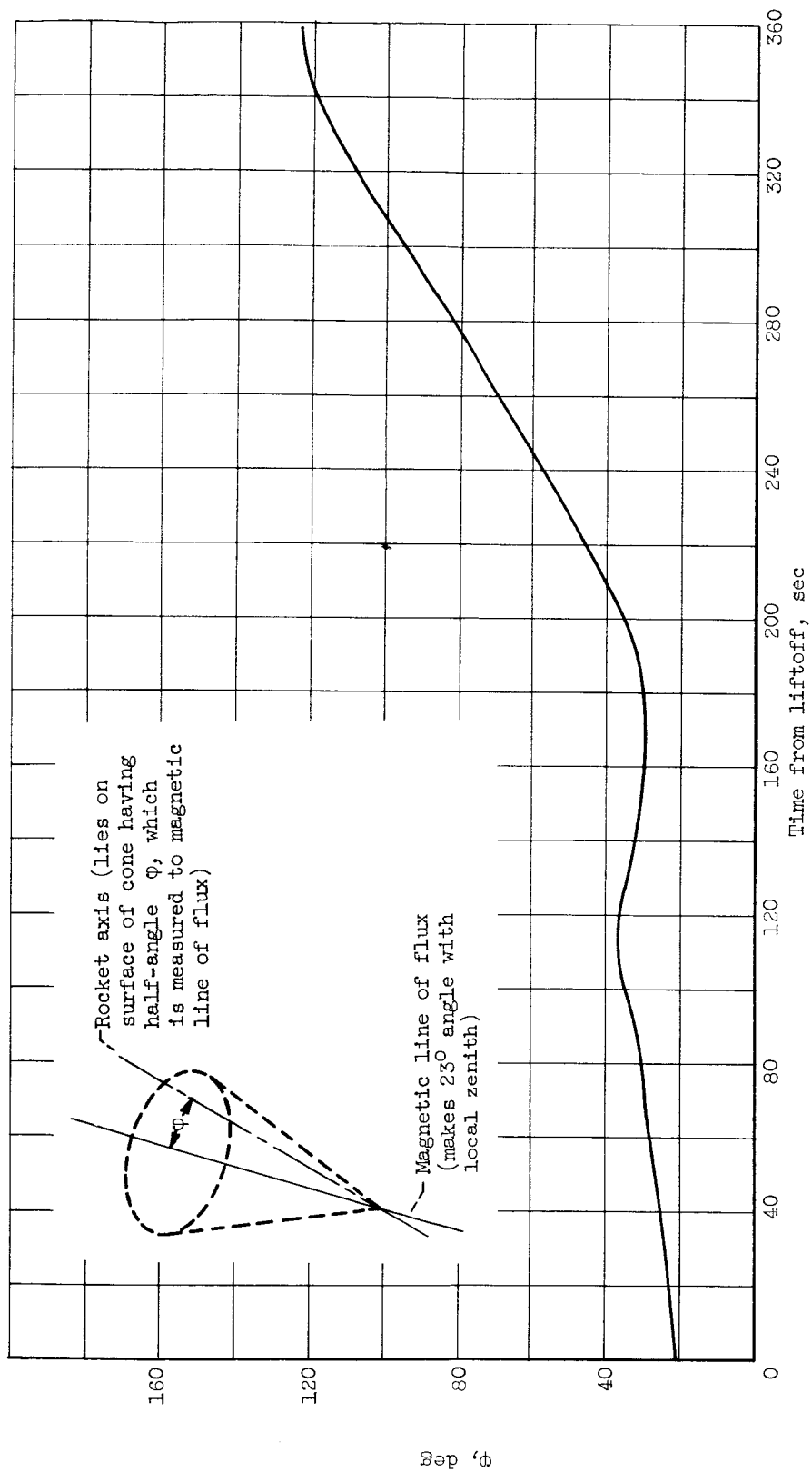
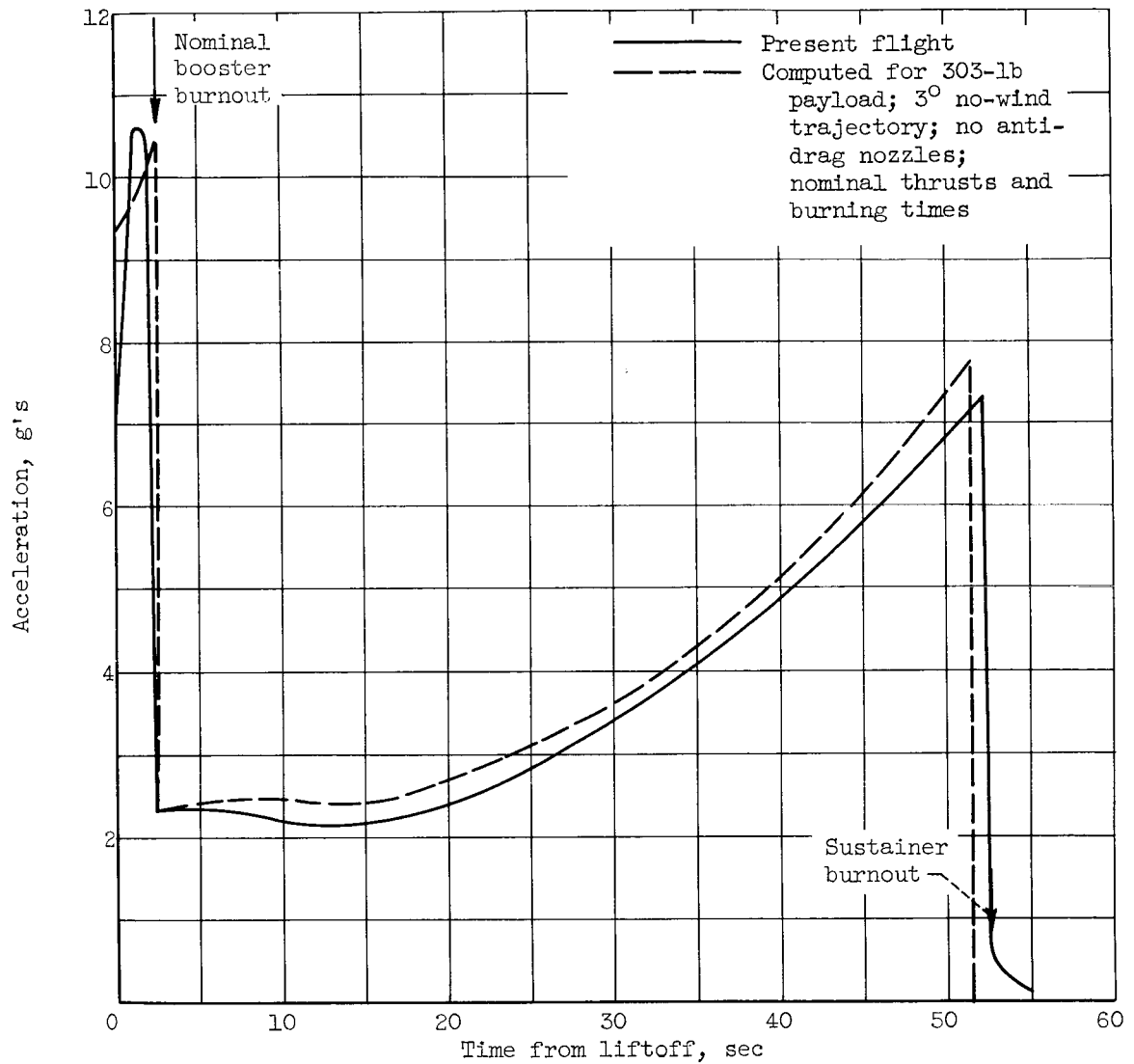


Figure 17. - Output from longitudinal magnetometer corrected for sudden changes of known cause.

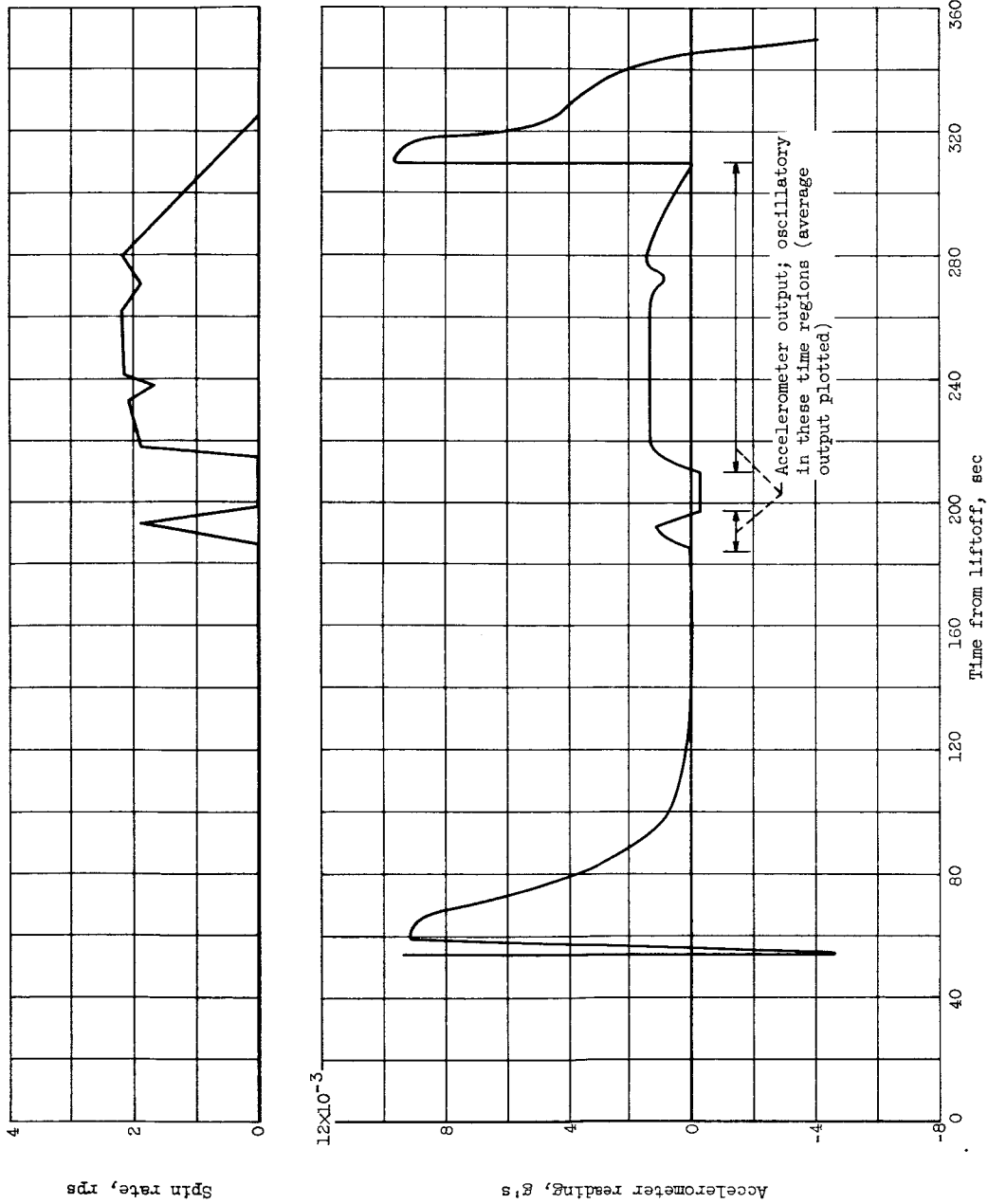
03712300

00



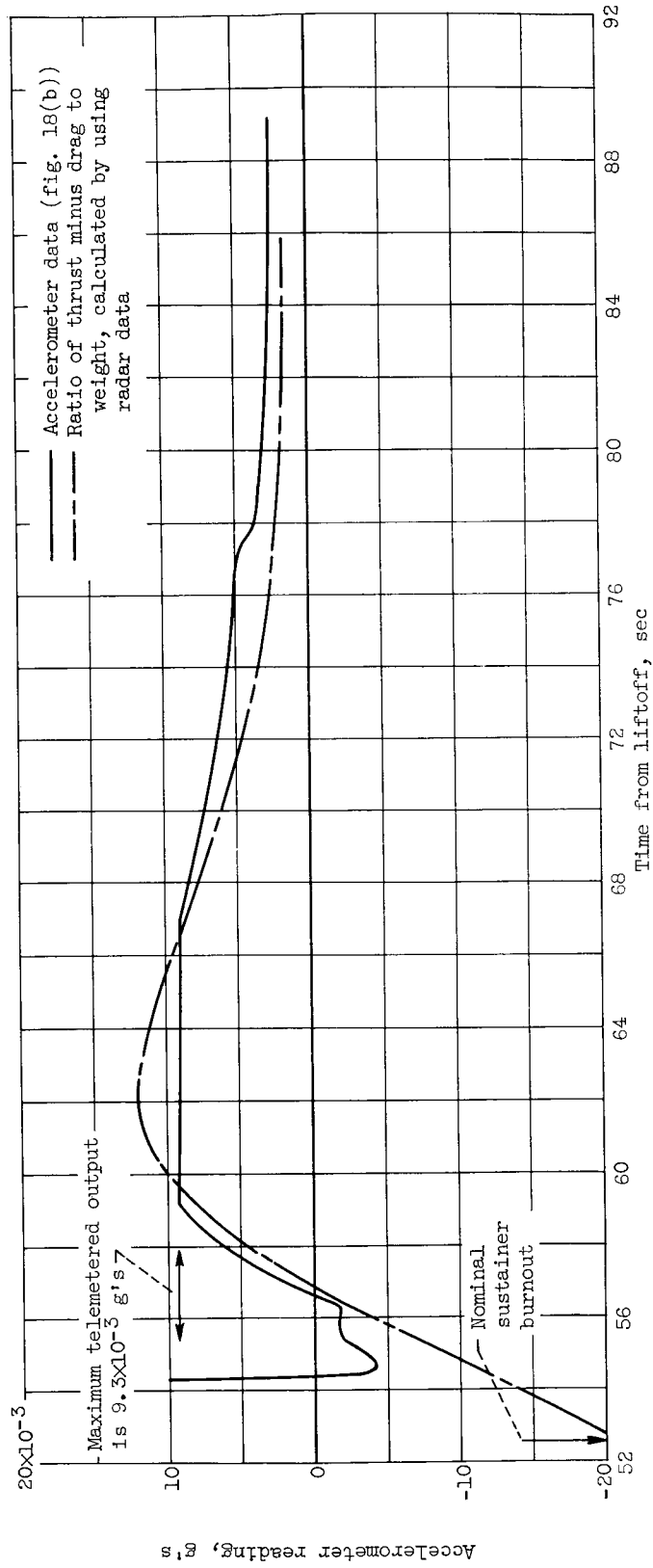
(a) During burning period.

Figure 18. - Longitudinal acceleration of rocket.



(b) Accelerometer output between 54 and 350 seconds after liftoff. Experiment spins counterclockwise as rocket comes toward viewer.

Figure 18. - Continued. Longitudinal acceleration of rocket.



(c) Accelerometer output from 54 to 89 seconds after liftoff.

Figure 18. - Concluded. Longitudinal acceleration of rocket.

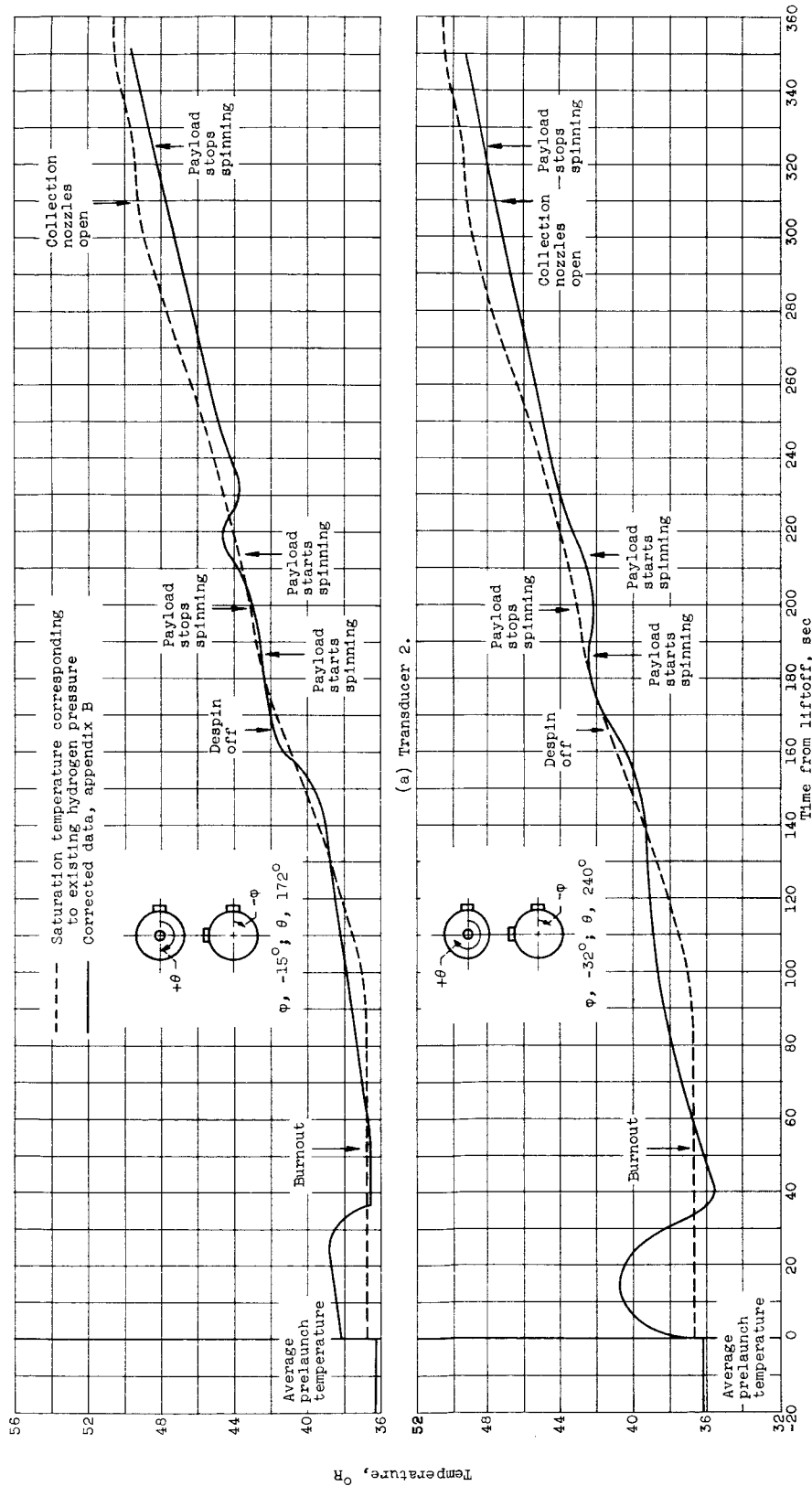
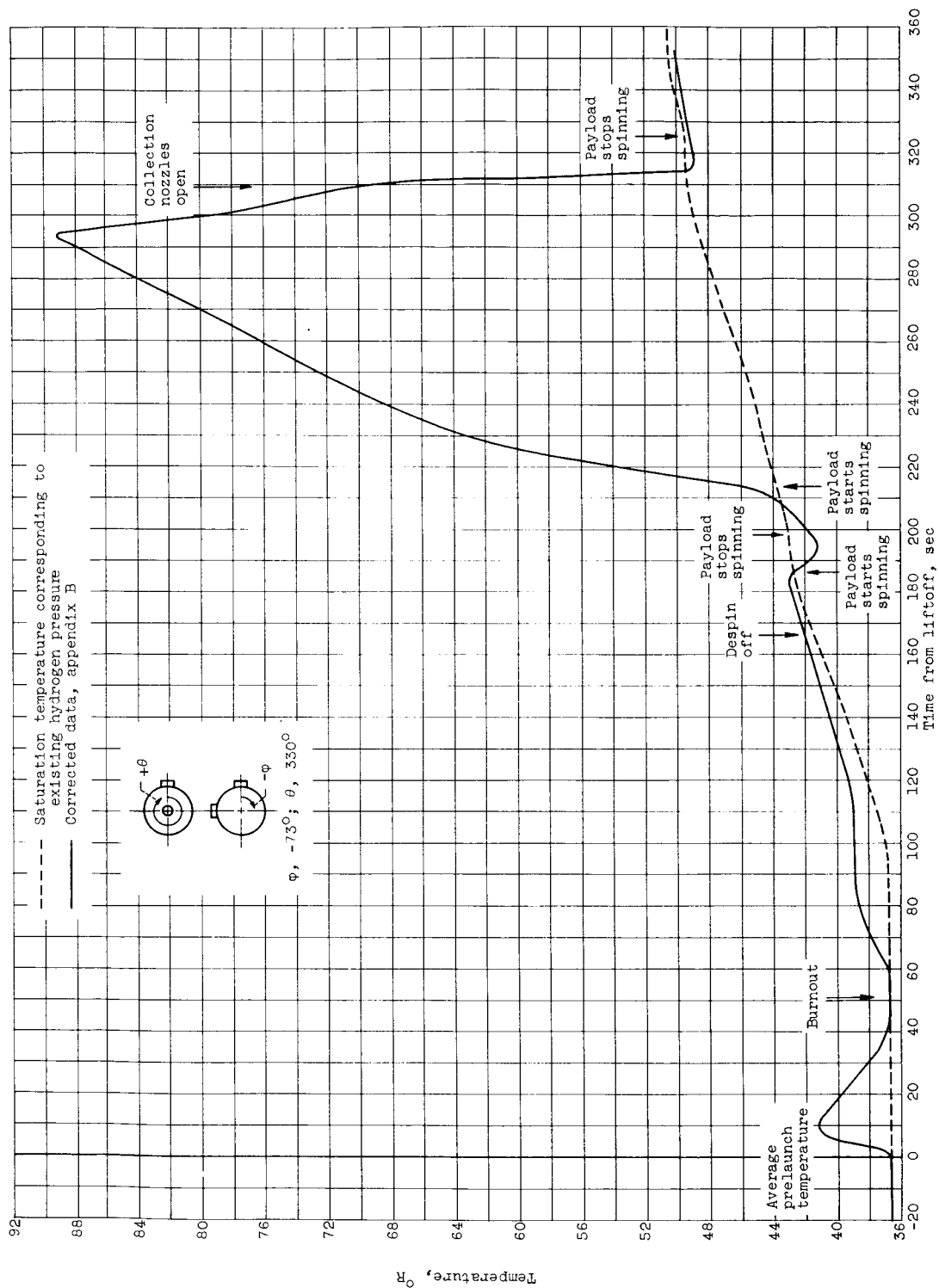


Figure 19. - Liquid-hydrogen-sphere wall-temperature history.



(c) Transducer 4.

Figure 19. - Continued. Liquid-hydrogen-sphere wall-temperature history.

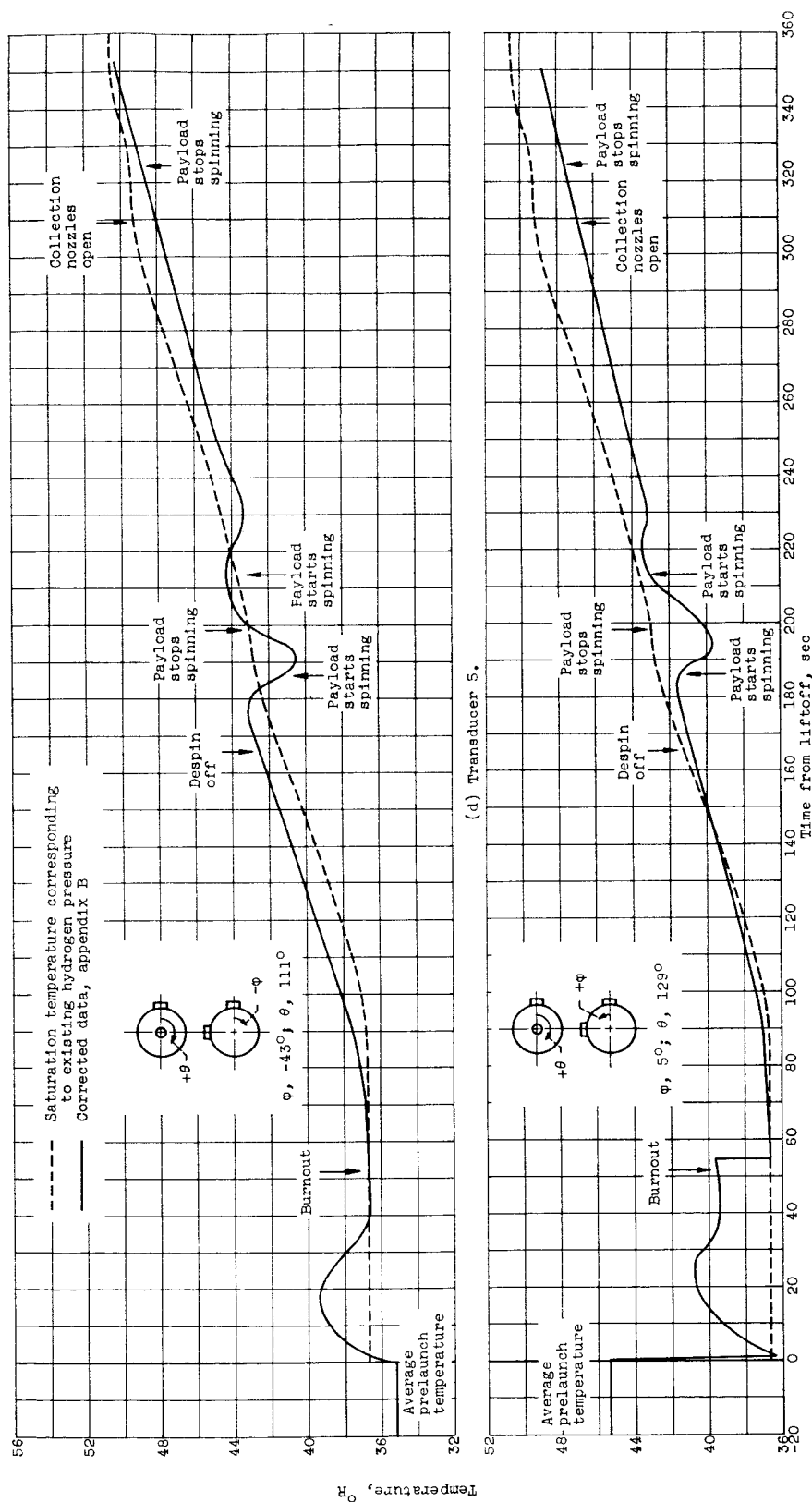


Figure 19. - Continued. Liquid-hydrogen-sphere wall-temperature history.

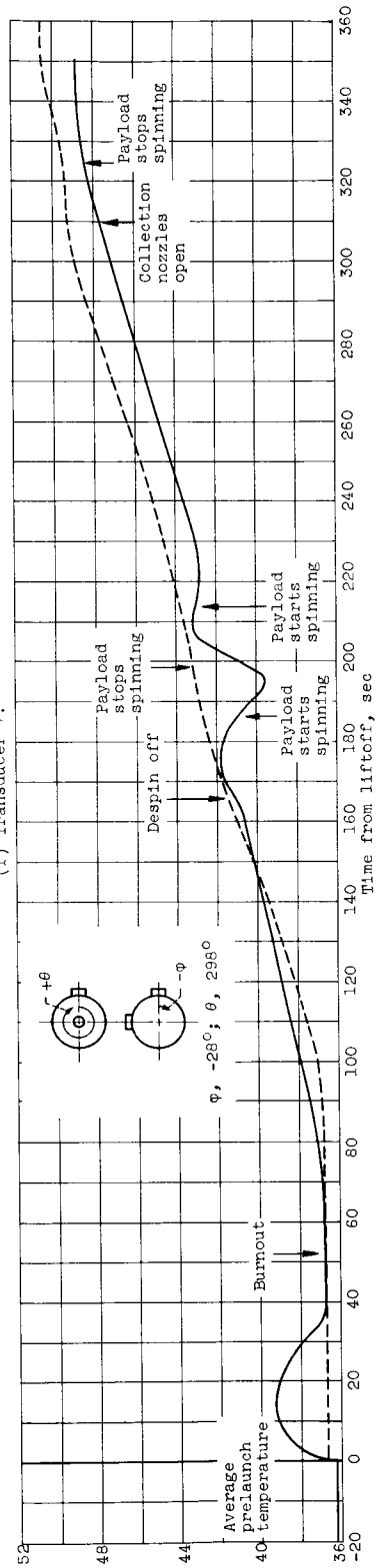
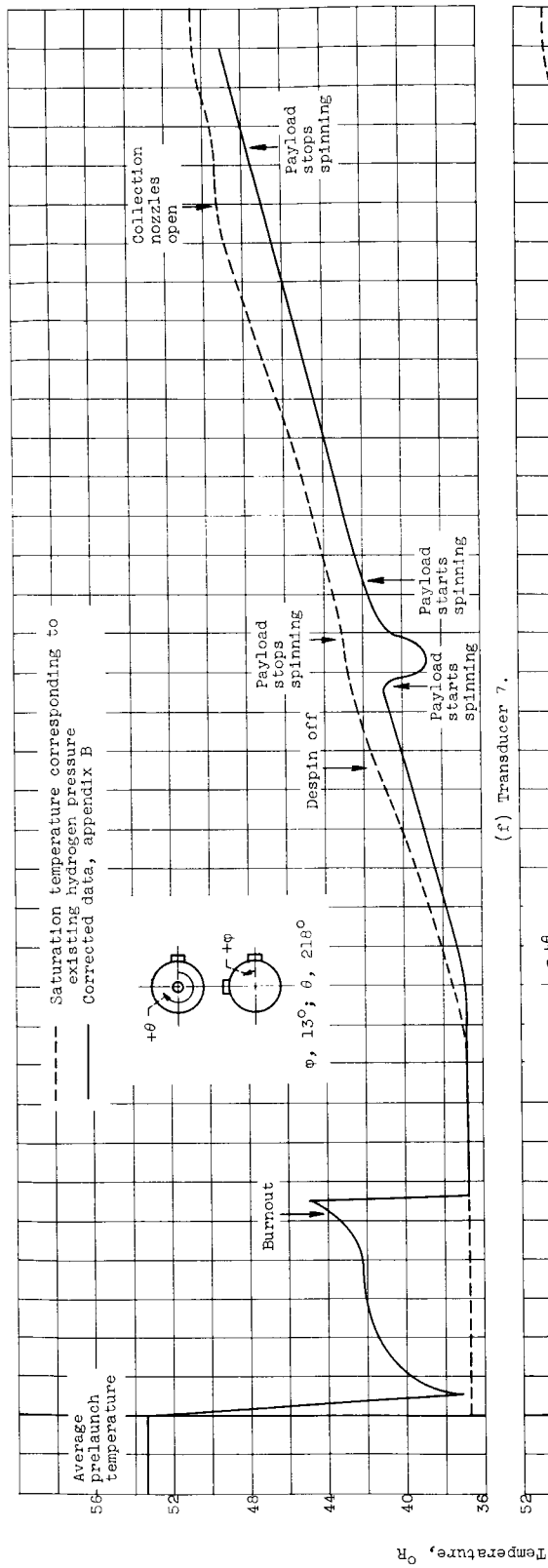


Figure 19. - Continued. Liquid-hydrogen-sphere wall-temperature history.

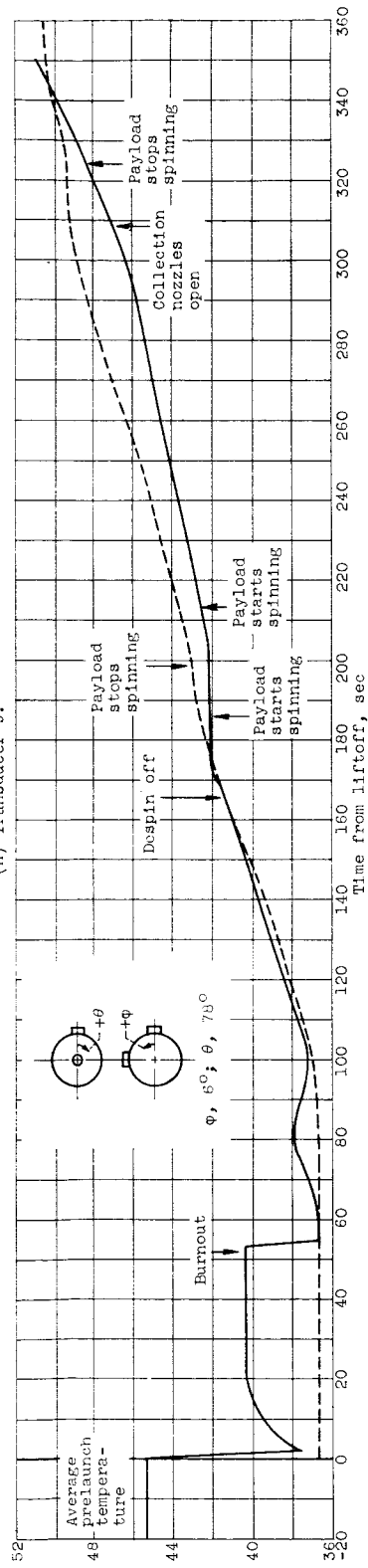
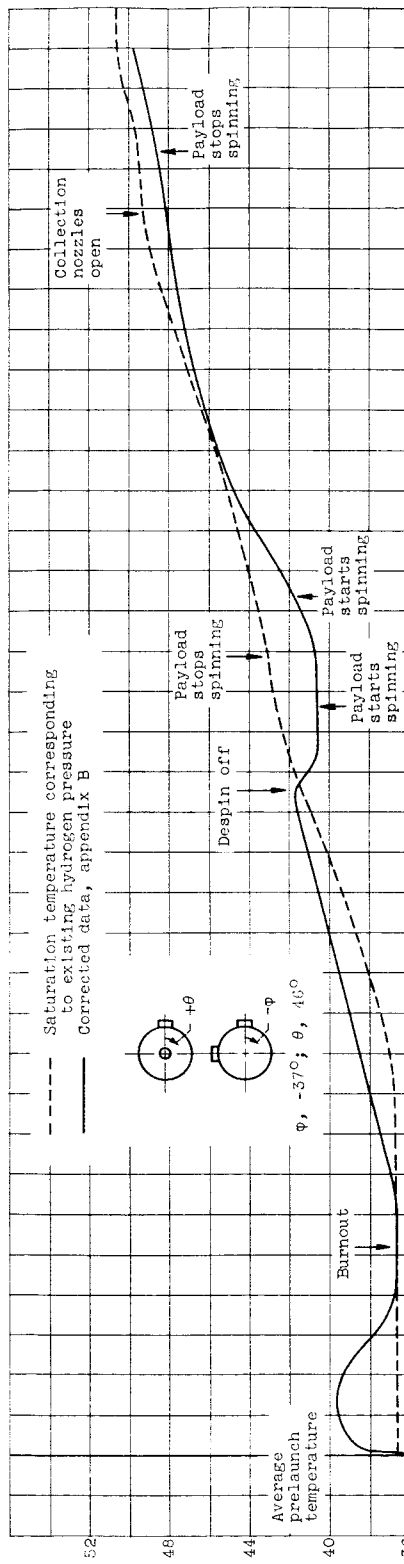
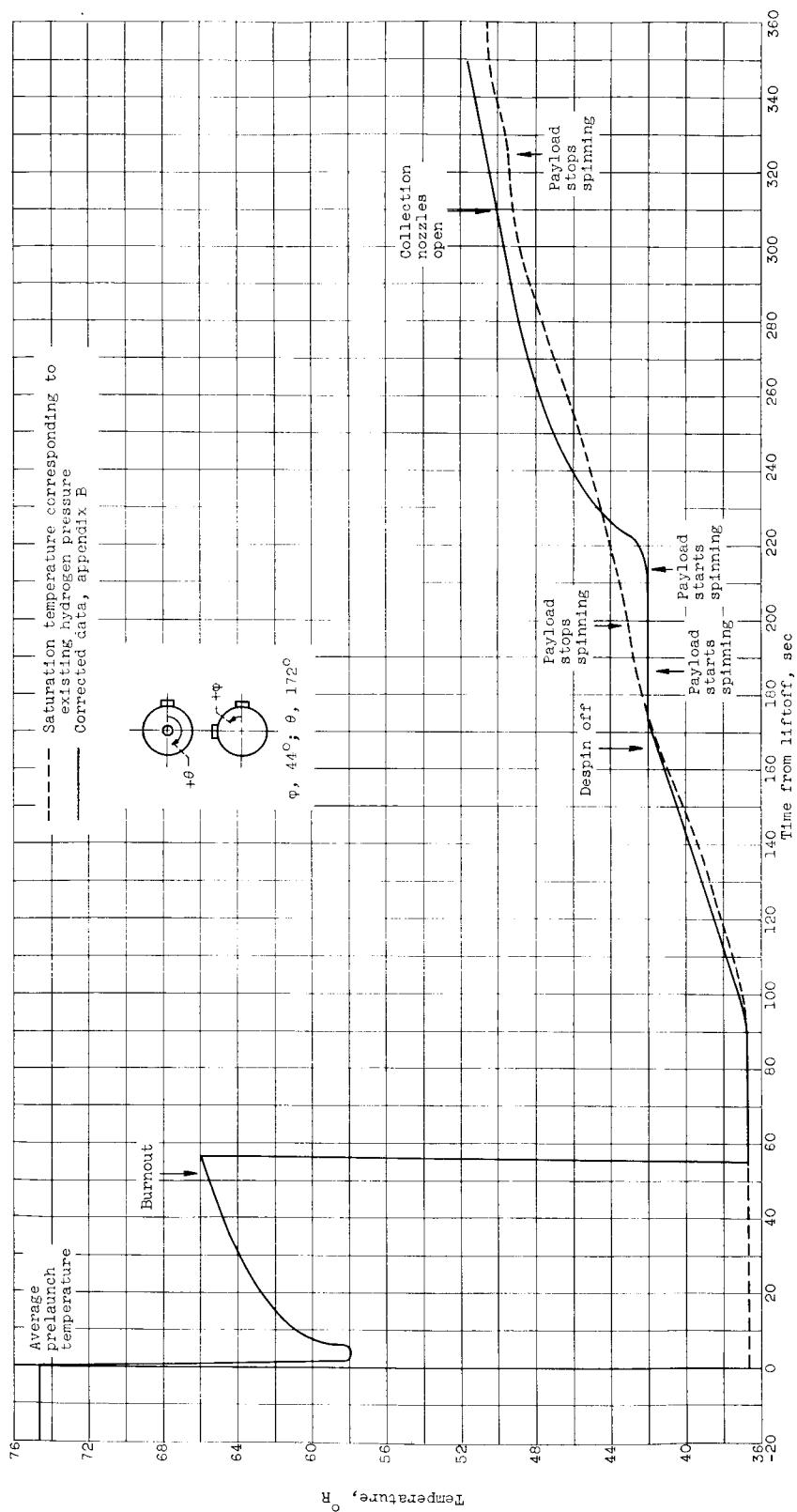
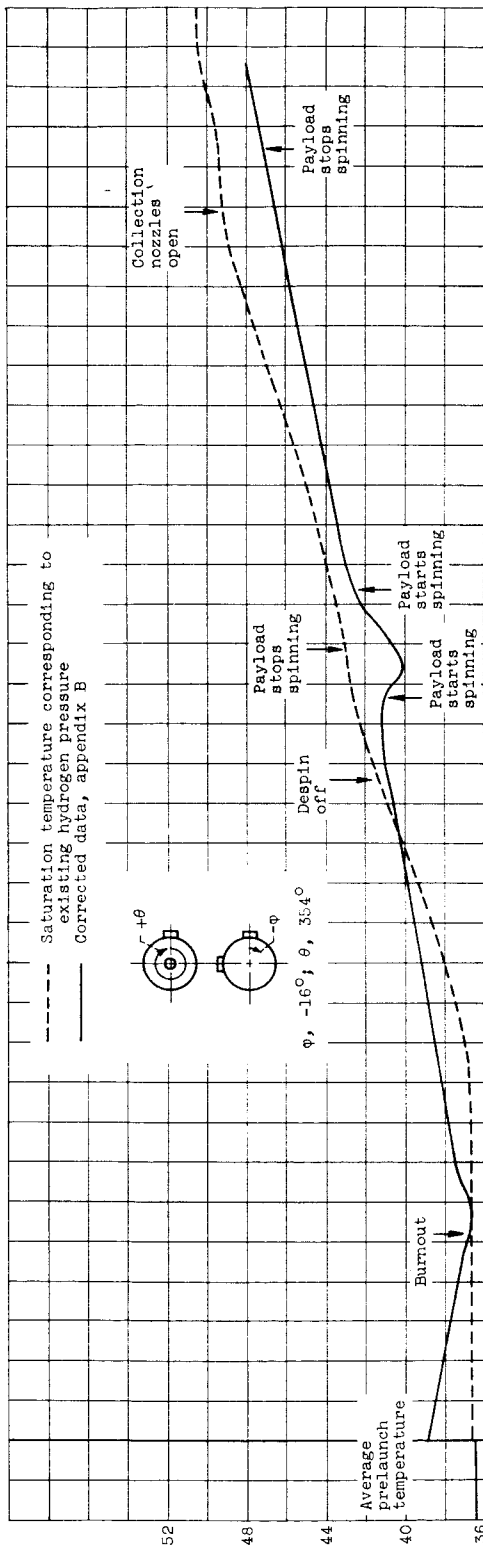


Figure 19. - Continued. Liquid-hydrogen-sphere wall-temperature history.

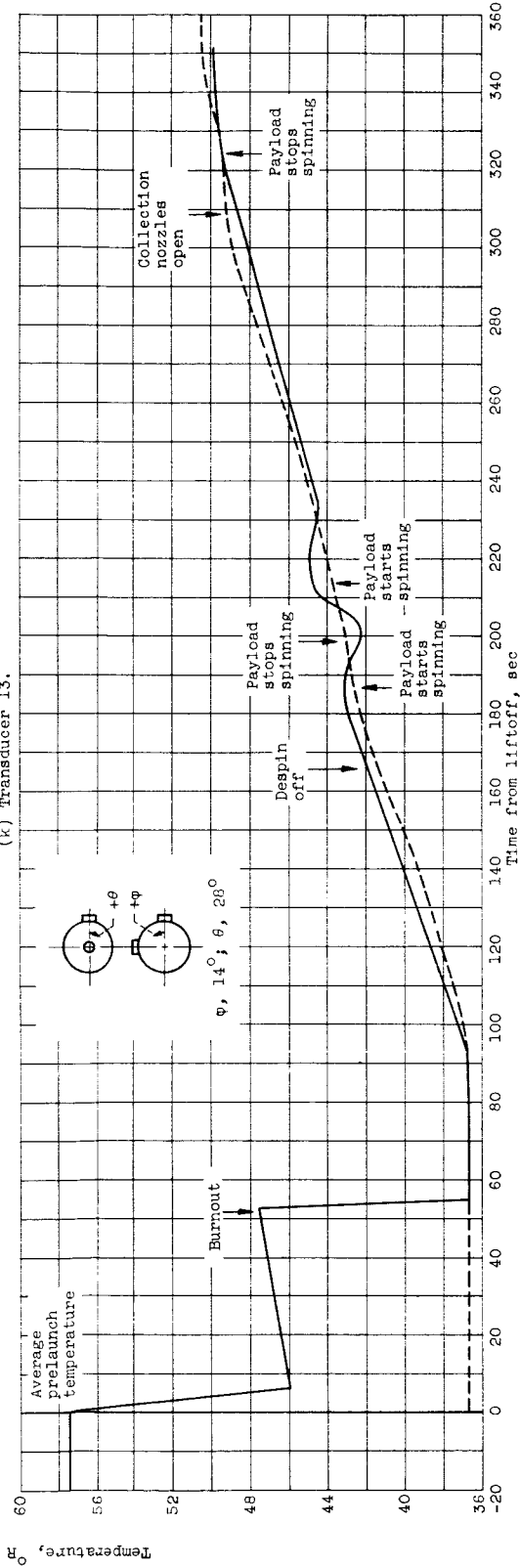


(s) Transducer 11.

Figure 19. - Continued. Liquid-hydrogen-sphere wall-temperature history.

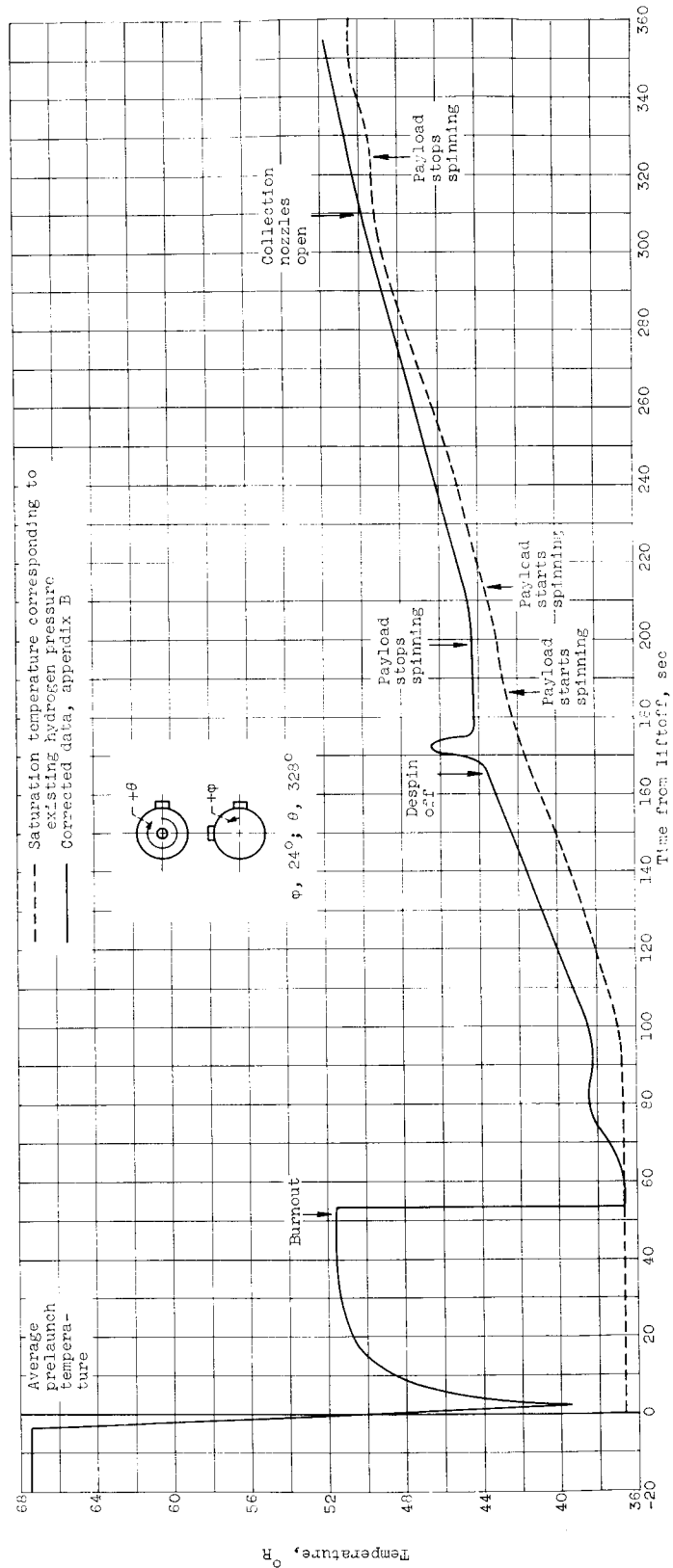


(k) Transducer 13.



(l) Transducer 14.

Figure 19. - Continued. Liquid-hydrogen-sphere wall-temperature history.



(m) Transducer 17.

Figure 13. - Continued. Liquid-hydrogen-sphere wall-temperature history.

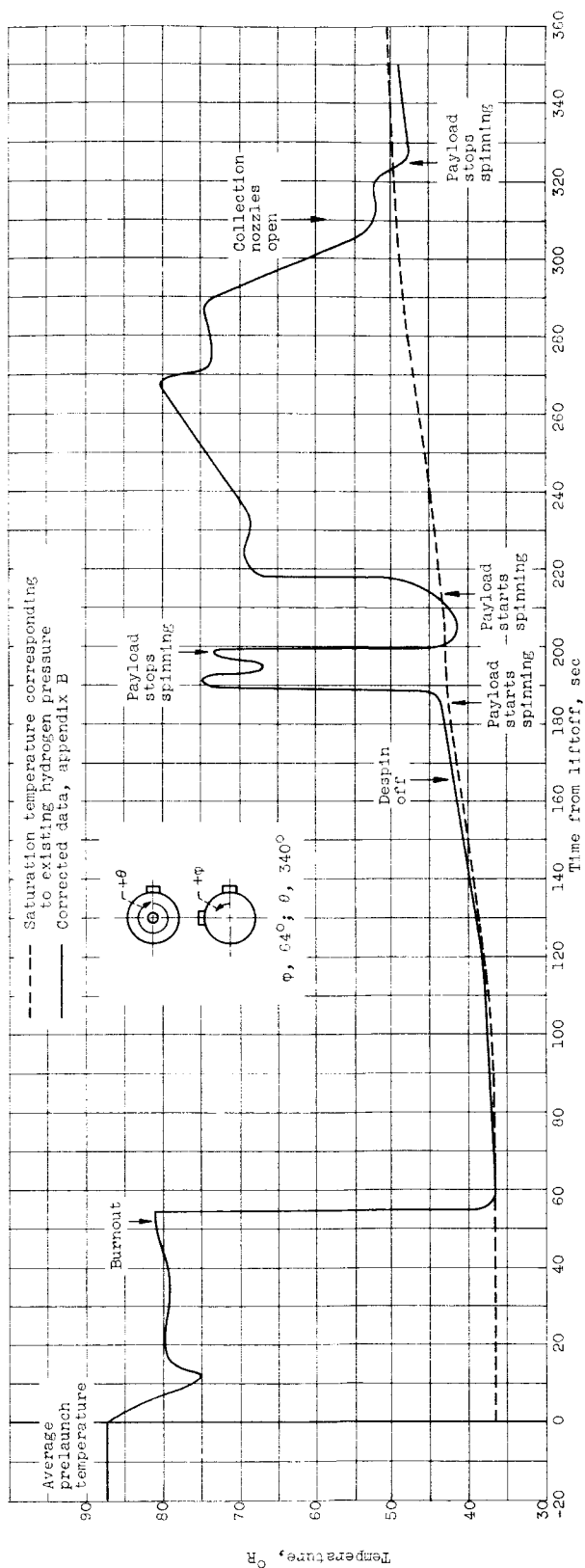


Figure 19. - Continued. Liquid-hydrogen-sphere wall-temperature history.

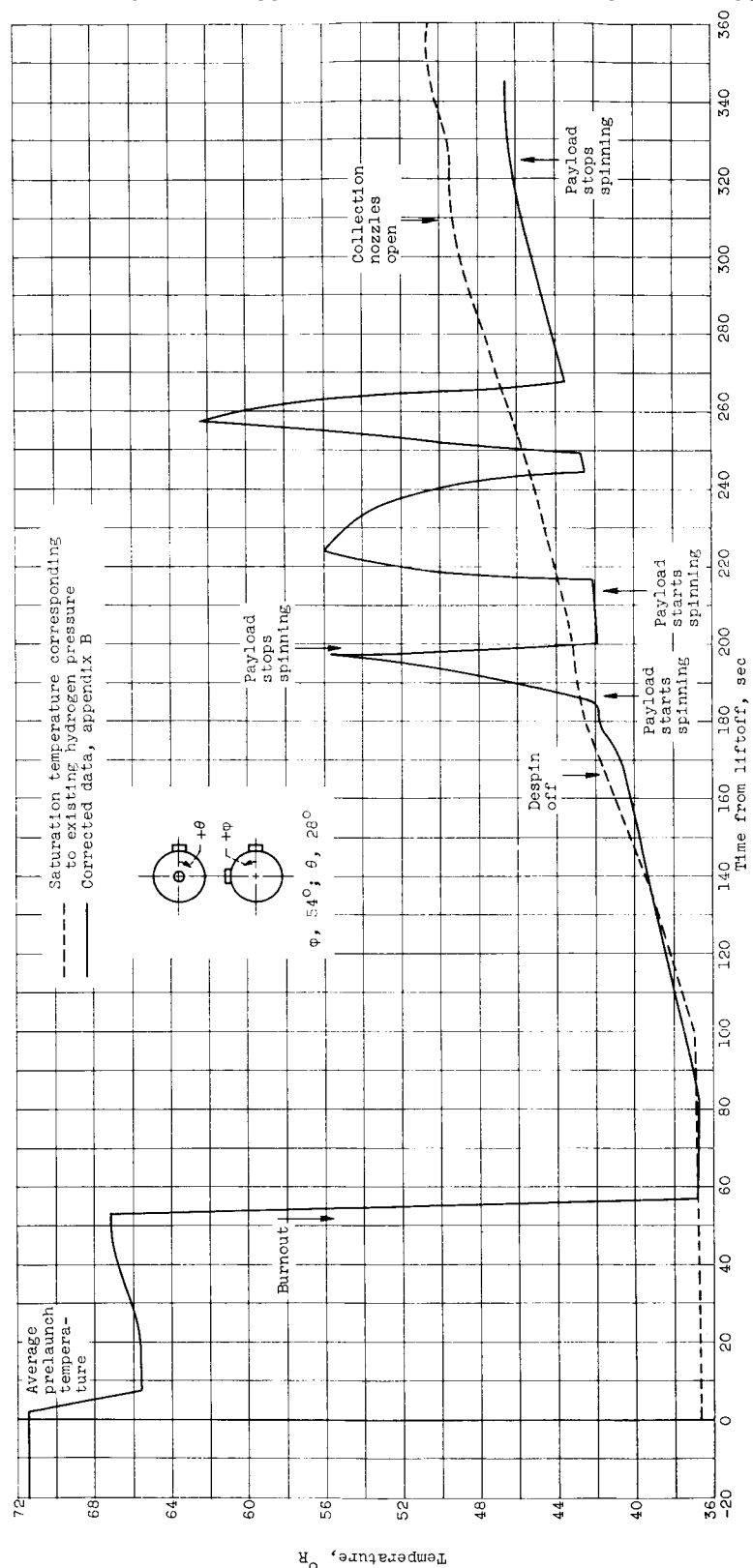


Figure 19. - Continued. Liquid-hydrogen-sphere wall-temperature history.

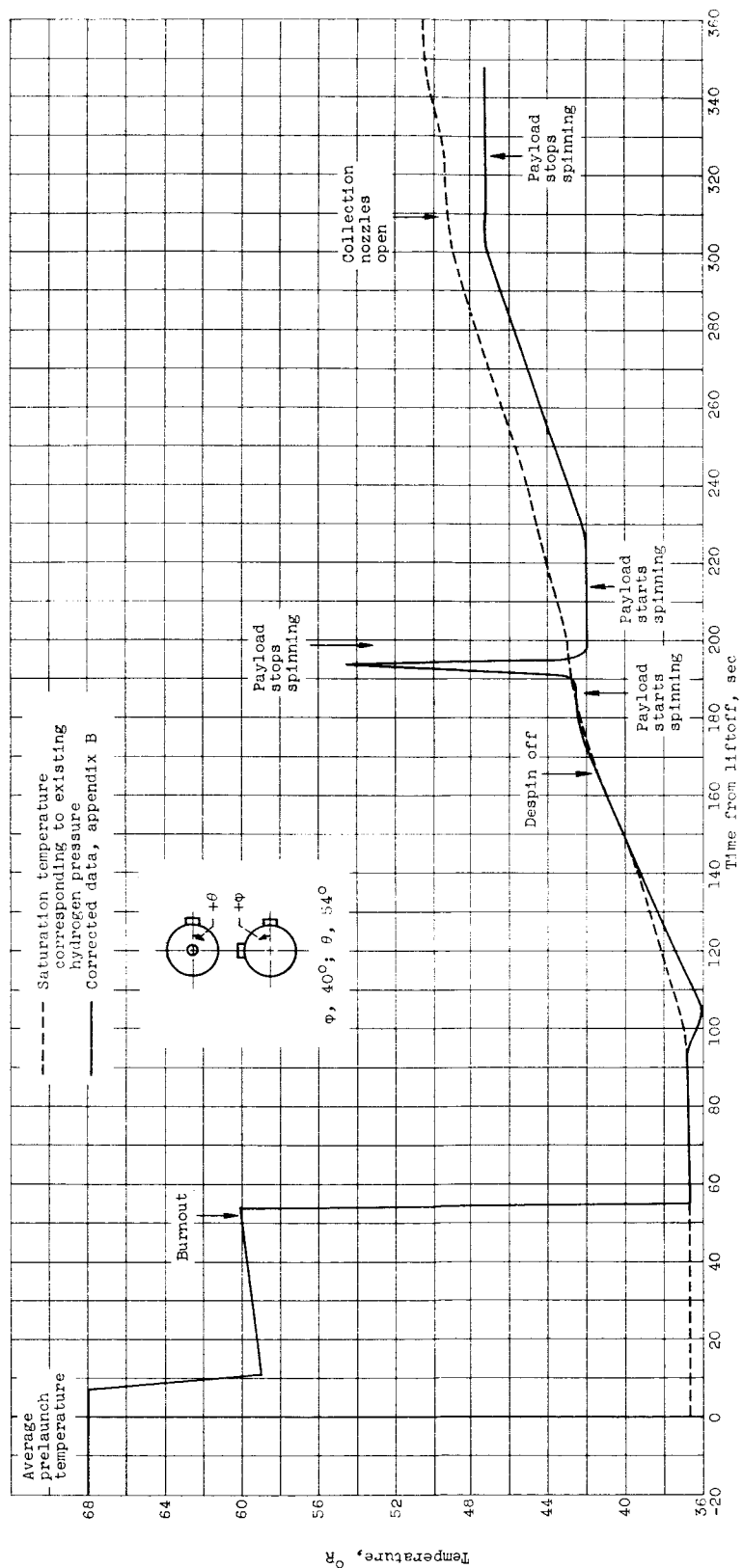


Figure 19. - Continued. Liquid-hydrogen-sphere wall-temperature history.

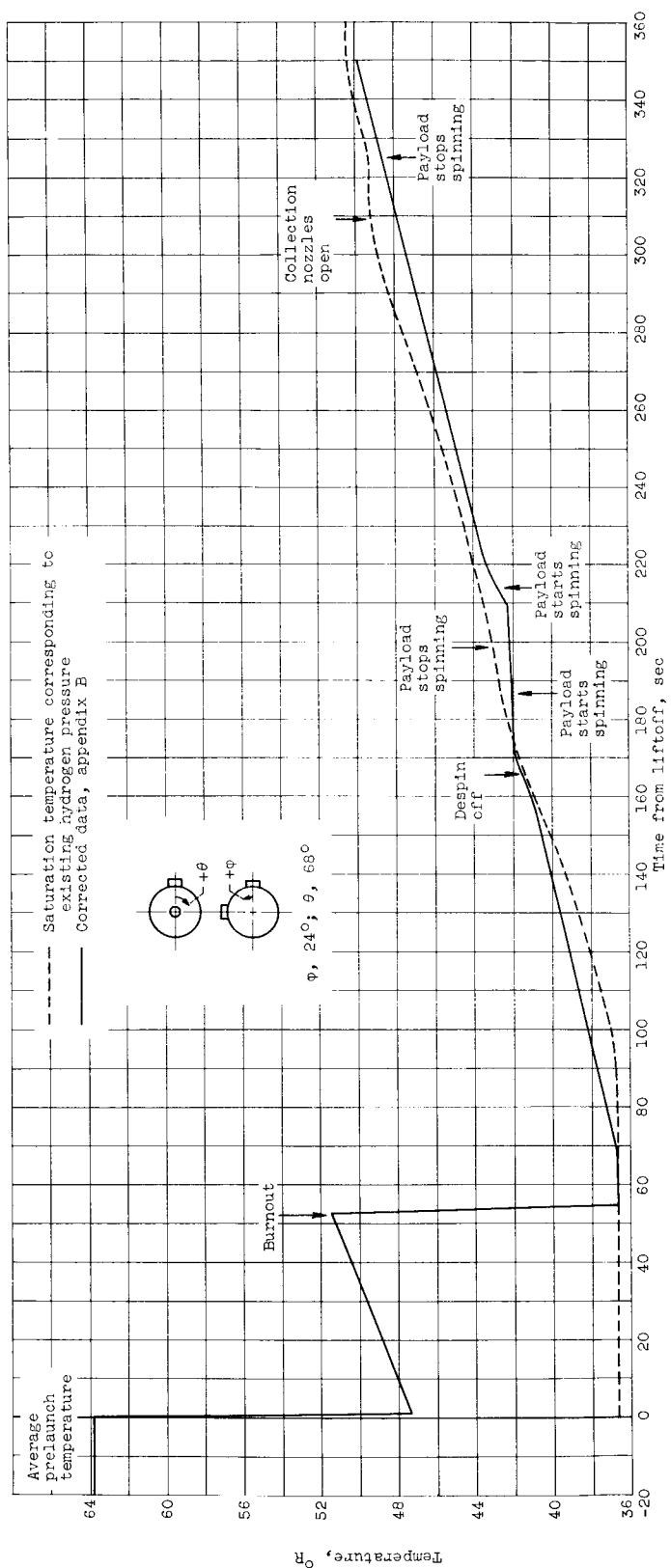


Figure 19. - Continued. Liquid-hydrogen-sphere wall-temperature history.
(q) Transducer 21.

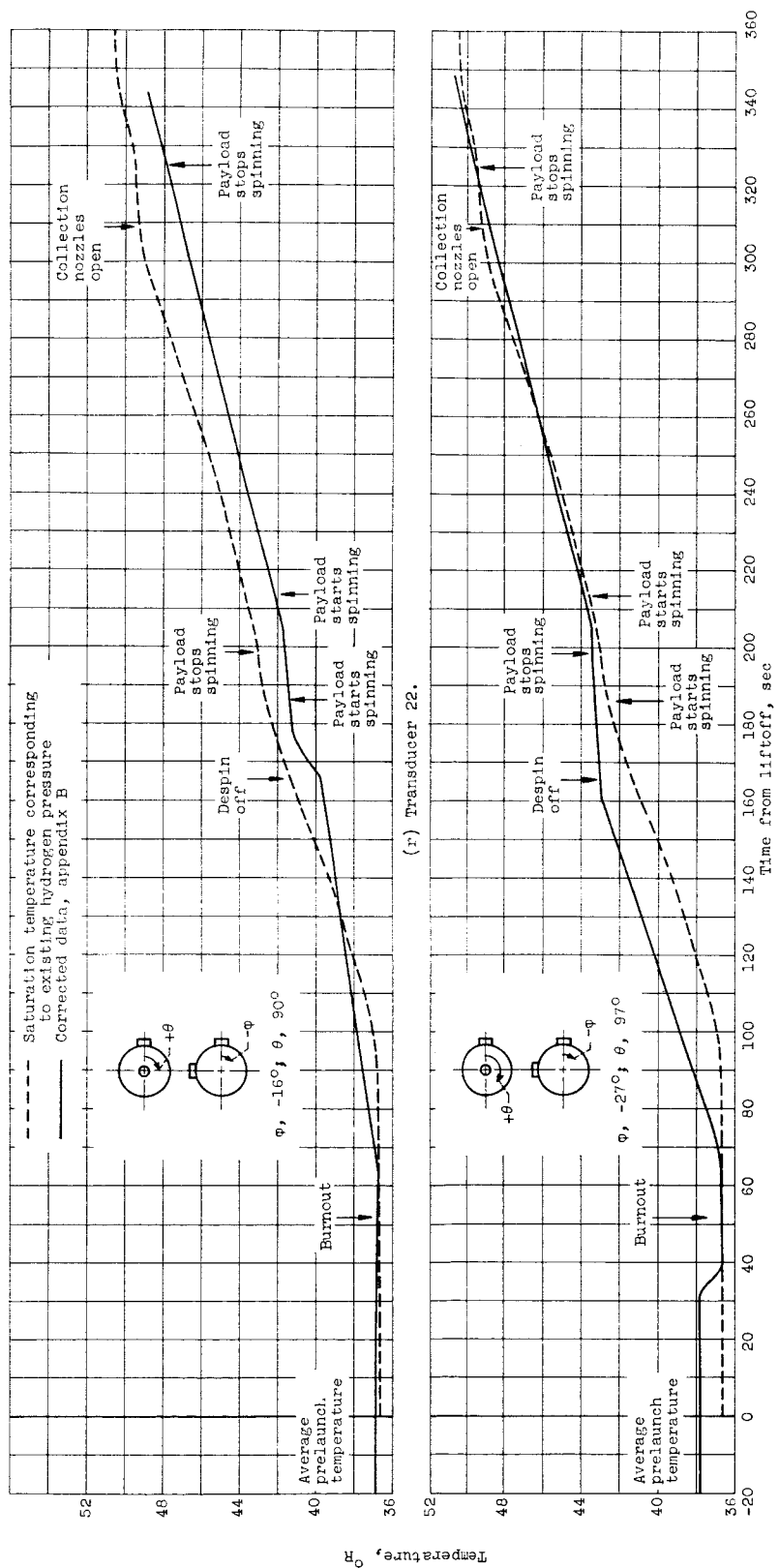
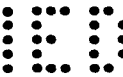
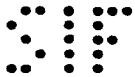


Figure 19. - Concluded. Liquid-hydrogen-sphere wall-temperature history.